PRESIDENCY UNIVERSITY

DEPARTMENT OF LIFE SCIENCES

PhD Thesis Synopsis

Title: **A study of antibacterial and anti-inflammatory activity of zinc oxide nanoparticles (ZnONPs) on multiple antibiotic resistant *Staphylococcus aureus* induced inflammatory rat model.**

Name of Candidate: **Sushmit Mukherjee**

Registration Number with date: **R-14RS18110020 (Date: 05th May 2016)**

Name of Supervisor: **Dr. Mausumi Sikdar (nee Bhakta)**

Name: Sushmit Mukherjee

Supervisor: Dr. Mausumi Sikdar (nee Bhakta)

Title of Thesis: A study of antibacterial and anti-inflammatory activity of zinc oxide nanoparticles (ZnONPs) on multiple antibiotic resistant *Staphylococcus aureus* induced inflammatory rat model.

PhD registration Number with date: R-14RS18110020 (Date: 05th May 2016)

Enrolment Number with date: SC/DOC/13-14/160

Place of work: Presidency University

Residential Address: 37/1 Naktala, Kolkata-700047, West Bengal, India.

Corresponding Address: 251 NSC Bose Road, Dakshini Appartment, Kolkata-700047, West Bengal, India.

Email: sushmitscience@gmail.com

Phone Number: 9477366056

18.10.2021

Signature of Research Scholar

18.10.2021

Signature of Supervisor

Contents

SERIAL NUMBER	CONTENTS	PAGE NUMBER
1	Abstract	4
2	Introduction	5 to 7
3	Objectives	8
4	Methodology	9 to 19
5	Results	20 to 42
6	Conclusion/Discussion	43 to 44
7	Significance of Study	45
8	Future Directions	46
9	Reference	47 to 55
10	Plagiarism Certificate	56
11	Additional Documents	57 to 62

I. Abstract

Conventional treatment strategies involving antibiotics are gaining accelerated challenges as a result of increasing antibiotic resistance by pathogenic microorganisms. A significant quantity of therapeutic research had been focusing in implementing green synthesized nanoparticles. In this study, green synthesis method has been used to prepare ZnONPs from leaf extract of coriander. The green synthesized and chemically synthesized commercially available ZnONPs showed almost no variation with respect to their size and morphology when characterized by methods like XRD, DLS etc. Comparison of anti-bacterial potential among both types of ZnONPs, used against strains of *S. aureus* (Control and Clinical) reveals, lower MIC and MBC of green ZnONPs was required to generate same quality of bactericidal effect as achieved by using the commercial one. This clearly signifies that, apart from easy synthesis procedure, lower doses are enough to generate the desired anti-bacterial efficacy. After inducing septic arthritis by clinical strain (KC-02) of *S. aureus*, both ZnONPs (chemical and green) were capable in lowering the increased serum level of inflammatory markers, without producing measurable amount of serum oxidative stress. The combination of ZnONPs (both chemical and green) and antibiotic shows excellent anti-bacterial and anti-inflammatory potential. The part of this study involving in-vivo model indicates that, both the ZnONPs when used in the mentioned concentration alone, and also in combination to antibiotic, are incapable of precipitating histological changes in selected organs like liver, kidney, spleen and adrenal gland. Therefore, use of ZnONPs, preferably green one for treating inflammatory disease like septic arthritis, could be a better choice over conventional antibiotic therapies.

II. Introduction

Nanomaterial intensified their acceptance in the field of biomedical research due to their extensively tiny size and unique properties [1]. Among several metal oxides, ZnONPs draws attention for its unique electrical, optical, and chemical properties. Large excitation binding energy and band gap (3.3mV), high electron mobility and high transparency enable it critically to serve the field of diagnostics, drug delivery, bio-molecular detection, DNA labelling, optoelectronics, biosensors, solar cells, cement ceramic sensors [2] etc. In addition, purification of water by removal of impurities such as, sulphur, arsenic along with waste water treatment also prospered by application of ZnONPs [3]. Among various metal oxide nanoparticles studied for antibacterial competency, zinc oxide nanoparticles (ZnONPs) and silver nanoparticles have exhibited prominent efficacy. Along with antibacterial potential, selective toxicity on bacteria and minimal effect on human cells [4] are accepted features of these nanoparticles. Excellent antibacterial activity of ZnONPs have also been reported against high temperature and pressure resistant spores [5] apart from its anticancer potential [6]. As per the reports, silver nanoparticles show maximum inhibitory effect on *Escherichia coli* and least on *Staphylococcus aureus* (*S. aureus*) [7]. Electrostatic adsorption of the nanoparticles to the bacterial surface and formation of hydrogen peroxide are considered to be the reason of efficient antibacterial activity of ZnONPs [8]. Based on this potent antibacterial efficacy, ZnONPs gained enough advantage in the arena of food and wood preservation, wound dressing, nano-medicines, cosmetics and disinfectant agents. These innumerable numbers of applications of ZnONPs build up the demand for different synthetic strategies [9]. Till date, multiple chemical and physical synthesis procedures are reported, of which all comprised of hazardous chemicals, resulting in usage of toxic substances. In addition, performing these synthesis protocols are tedious and expensive [10]. Acceptability of microorganism-based synthesis procedure could have been universal, if the criterion of maintaining highly aseptic conditions were avoidable [11]. Besides, necessity of conducting several purification steps has become a major hindrance for application at industrial scale [12]. Green synthesis emerged as an inexpensive and eco-friendly alternative for synthesis of well structured, biocompatible and potent ZnONPs [13]. Several plants such as *Azadiracthta indica, Cassia auriculata, Ocimum sanctum, Aloe vera, Coriendrum sativum* etc., have been exploited for synthesis of ZnONPs from extract of their different parts [14]. It is known that the plants have high concentrations of active compounds like methylxanthines, phenolic acids, flavonoids

and saponins [15]. These compounds are more known as antioxidants as they can neutralize reactive oxygen species (ROS) and free radicals and chelate metals [16]. Hence, the antioxidants present in the plants are possibly responsible for the green synthesis of metal or metal oxide nanoparticles due to their capability to bio-reduce or chelate metal ions and to act as stabilizers of the synthesized nanoparticles [17].

Staphylococcus aureus (*S. aureus*) is considered one of the main infection-causing pathogens found in both hospital and community [18]. The range of infections caused by these bacteria includes mild skin and soft tissue infections, infective endocarditis, osteomyelitis, bacteremia, fatal pneumonia and many more [19]. *S. aureus* does not form spores or flagella, but possesses a tough capsule, and are capable of producing golden yellow pigment and also decompose mannitol [20]. Additionally, as it gives positive result when test of plasma coagulase, lactose fermentation and deoxyribonuclease are done, therefore, strain identification can commonly be done using these methods [21]. Its multi-drug resistance phenotype makes it an important member of target-pathogen-family in the history of antibiotic chemotherapy. Almost all well-known antibiotics developed since 1940s are ineffective against *S. aureus*. MRSA among clinical isolates of *S. aureus* was first isolated in 1961 [22]. Then MRSA gained world-wide importance as a multi-resistant hospital pathogen. In 1997, vancomycin susceptible MRSA (strain Mu50) was successfully isolated [23]. In order to overcome these problems, investigators are in constant search of an alternative to conventional antibiotics [24].

Septic arthritis can be categorized as a true rheumatologic emergency which may progress to disability or death of an individual. Gram-positive organisms are mostly found responsible for precipitating septic arthritis [25]. *S. aureus* is the most common causative organism of septic arthritis. Number of adhesins produced by *S. aureus* can easily bind to extracellular matrix proteins. Bacterial invasion results in release of bacterial enzymes and toxins, followed by host inflammation and tissue ischemia commonly lead to septic arthritis induced damage of cartilage and joints [26]. Outcomes of septic arthritis are prominently visible in human population of which osteomyelitis occurs in 27% to 46% and mortality in 7% to 18%. Patients experiencing fever, rigors, swollen with painful joint are also common symptoms enabling easy and straight forward diagnosis of septic arthritis [27]. Although joints are primary target of this infection, majority cases are concentrated on the knee joint, that is forty-five percent. Rest of the joints like hip (15%), ankle (9%), elbow (8%), wrist (6%), and shoulder (5%) also experience infection

induced damage due to septic arthritis in adults [28]. White blood cell (WBC) count in synovial fluid exceeding 50,000 cells/mm^3 in patients of septic arthritis seek empirical treatment. In case of treating immunosuppressed patients, other indicators of septic arthritis should be given higher priorities, as their normal synovial fluid WBC count is low [29]. Antibiotic courses normally prescribed for not-so-severe bacterial arthritis ranges from 3 to 4 weeks but if imaging evidences does not indicate complete amelioration, antibiotic treatment must continue for at least 6 weeks [30].

III. Objectives

1. Characterization of ZnONPs with respect to their size, mass, etc.
2. Development of inflammatory rat model induced by multiple antibiotic resistant *S. aureus.*
3. Study of the antimicrobial and anti-inflammatory effect of ZnONPs on the inflammation model.

IV. Methodology:

A. SYNTHESIS OF ZnONPs

1. Commercial Zinc oxide nanoparticle

The commercially available zinc oxide nanoparticles were purchased from Sigma (Aldrich-721077-100G).

2. Green Synthesis of Zinc oxide nanoparticle

Extract preparation: Fresh coriander (*Coriandrum sativum*) leaves were first thoroughly washed with Millipore water and kept at room temperature until properly dried. Then, 25gm of leaves were boiled at 80°C in 100 ml deionized water for 20 minutes. Next, cooling and filtration was performed and the filtrate was collected in a sterile container [31].

Preparation of salt solution: 0.2 M Zinc acetate solution was prepared using 2.2 gm of zinc acetate ($ZnC_4H_6O_4$) powder and 50 ml Millipore water, followed by stirring with a magnetic stirrer, until dissolved entirely [32].

Nanoparticle formation: At room temperature, 50 ml of prepared Zinc acetate solution (0.2 M) was kept at stirring condition followed by addition of 50 ml filtered coriander leaf extract. 10 ml, 1 M NaOH was poured drop wise into this solution. A characteristic yellowish white precipitate was instantly visible after the addition of NaOH solution [33].

B. CHARACTERIZATION OF ZnONPs

1. Characterizations of both green synthesized and Commercial ZnONPs

Powder X-ray diffraction method was employed to investigate the crystal structure of synthesized and commercial ZnONPs. This study was done by X-ray powder Diffractometer [34] model D8, Bruker AXS, Wisconsin (USA), containing Cu-Kα as a target, employing 1.5418 Å wavelengths within 20°- 80°2θ range, and a scan speed of 1 s/step was maintained while operating at 35kV.

To ascertain the functional groups, present in the used spice extract, Fourier transform infrared spectroscopy (FTIR) analyses was carried out. A range from 400 cm^{-1} to 4000 cm^{-1} was studied [35] by FTIR-8400S, Shimadzu.

The stability and particle size distribution of synthesized ZnONPs and the commercial one was evaluated by the help of DLS (Dynamic light Scattering) study [36] conducted by Zetasizer (NANO ZS90, Malvern Instruments Ltd., UK).

Finally, to verify the morphology of both green synthesized and commercial ZnONPs, field emission Scanning Electron Microscopy (FE-SEM) [37,38] was performed through INSPECTF50 (FEI, Netherland).

C. COLLECTION AND IDENTIFICATION OF CLINICAL STRAIN OF *S. aureus*

1.* Source of Collection of bacterial strains of *S. aureus

Clinical strains of *S. aureus* were collected from Calcutta School of Tropical Medicine, Kolkata (Permission letter attached) and subjected to both biochemical and molecular tests for identification. The study including the clinical strain of S. aureus was conducted with permission, provided by Institutional Biosafety Committee of Presidency University (BT/BS/17/536/2013-PID).

2. Biochemical Assay

After collection, the bacterial strains (clinical) were cultured on nutrient agar media containing 10% NaCl. Next, the bacterial colonies were stained by Gram staining method [39, 40]. Results of Gram staining was obtained after imaging appropriate fields observed at 10X (Compound Microscope). In order to perform catalase test [41], bacterial colonies were used to prepare smear in clean and sterile glass slide. H_2O_2 was added to the bacterial smear to check whether the bacteria are catalase positive. Identification of *S. aureus* was done on the basis of these above tests. All the mentioned tests were also performed with the control strain of *S. aureus* (ATCC25923).

3. Molecular Assay

DNA Extraction: DNA of collected clinical strain of bacteria was isolated according to the manufacturer's protocol, provided by the kit (MB505, HiMedia, Mumbai). Briefly, the cell pellet obtained after centrifugation of 1.5 ml overnight bacterial culture was resuspended in lysozyme solution (45mg/ml) for 30 minutes at 37º C. 20 µl each Proteinase K (20 mg/ml) and RNase A (1mg/ml) along with 200 µl lysis solution were added to lyse the cells, following incubation at 55 ºC for 10 minutes. Then 100% ethanol was added to cell lysate before washing and elution of

DNA by adding elution buffer. Concentration of DNA was measured by Nanodrop Spectrophotometer (Thermo Scientific Nano Drop 2000)

Gene amplification by PCR: Amplification of 16S rRNA gene was done by PCR (Polymerase chain reaction) thermocycling process [42] (Model T100TM Thermal Cycler, Bio-Rad). PCR products were subjected for Sanger sequencing [43] followed by BLAST analysis of 16S rRNA gene with Gene Bank database (www.ncbi.nlm.nih.gov) for species identification.

D. DETERMINATION OF ANTIBACTERIAL POTENTIAL OF ZnONPs

1. Antibiotic susceptibility test

Both the control and clinical strains of *S. aureus* (ATCC25923 and KC-02) were exposed to multiple antibiotics to determine their profile of resistance to antibiotics. Disc diffusion method was implied for this study, in which standard antibiotic discs purchased from HiMedia were used. Fresh cultures of both the strains of *S. aureus*, (ATCC25923 and KC-02) were spread on Mueller Hinton agar plates. After 10 minutes, standard disc of respective antibiotics was placed at equidistant positions. Duplicate plates for both strains were incubated overnight. Next day, zone of inhibition was measured in millimeter [44, 45].

2. Determination of Minimum Inhibitory Concentration (MIC) for both commercial and green synthesized ZnONPs

On the day before the experiment, liquid cultures of each of the bacterial strains of *S. aureus* (ATCC25923 and KC-02) were prepared in sterile Mueller Hinton Broth. Graded concentrations of synthesized ZnONPs solution ranging from 0 μg/ml to 100 μg/ml were added to several tubes each containing 1ml sterilized Mueller Hinton Broth. Each tube was then inoculated by 10 μl bacterial culture containing 2.5×10^5 CFU ml^{-1} bacteria and subjected to overnight incubation at 37°C. This procedure was carried out with the commercial ZnONPs also, for both the strains of *S. aureus*. Optical density (at 530 nm) of the content of each tube was measured using spectrophotometer to determine minimum inhibitory concentrations [46].

3. Determination of Minimum Bactericidal Concentration (MBC) for both commercial and green synthesized ZnONPs

10 μl from each tube used for MIC study of both the strains of *S. aureus* (ATCC25923 and KC-02) containing ZnONPs treated bacterial cultures were further spread on nutrient agar plates. These

plates were then subjected to overnight incubation at 37°C. The result was observed on the next day, and the minimum concentration at which no bacterial colony was observed, was considered as the MBC value. In order to determine the MBC value of the commercial ZnONPs, the same procedure was followed for each bacterial strain [47].

4. Tolerance Level

Evaluated MIC and MBC values express the tolerance level of each bacterial strain against both the green synthesized and commercial ZnONPs with the help of the following formula [48].

MBC/MIC = Tolerance level

5. Agar Well Diffusion Method

Several tubes containing 1ml freshly prepared Mueller Hinton Broth were inoculated with each bacterial strain and kept for an overnight incubation at 37°C. On the next day, each grown bacterial cultures were diluted using sterile Mueller Hinton Broth to adjust the turbidity as per the standard of 0.5 Mac Farland (10^8 CFU/ml). From these diluted cultures, 100 µl were spread on a nutrient agar plate followed by punching of 4 wells in each plate measuring 0.563 cm diameter. To two of these wells, experimentally obtained MBC values of ZnONPs were added, (one well was filled with green synthesized and the other with commercial). Doxycycline (antibiotic) was added in a well as positive control and sterile distilled water was added in another well. These plates were kept for overnight incubation at 37°C. The obtained zones of inhibition were measured and compared [49].

6. Kinetics of bacterial growth inhibition

A series of five glass containers with sterilized Mueller Hinton Broth were prepared. Fresh bacterial culture of a strain was added to all containers leaving one, used to set blank during the measurement of optical density at 530 nm. The three containers were also provided with specific antibacterial agents like commercial ZnONPs (Sigma), green-synthesized ZnONPs (coriander leaf) and an antibiotic (Doxycycline), at pre-determined MIC values. Among four containers, one was deprived of any antibacterial agent and used as control for the experiment. These containers were then incubated at 37^0 C. These set of containers were prepared for both strains of *S. aureus* (ATCC25923 and KC-02). Optical density of the contents of each container was measured at an interval of one hour, starting from the zero hour (just before incubation). The

obtained values were used to plot the growth curve of both strains of *S. aureus* used for this study [50].

7. Bacterial Cell Viability Assay

3-(4, 5-dimethylthiazol-2-yl) -2, 5-diphenyltetrazolium bromide (MTT) was used in a standard protocol to determine the cell viability of bacteria. Bacterial cells were incubated overnight with different concentrations of both the synthesized and commercial ZnONPs at 37°C. Next day, bacterial cells were collected after performing centrifugation at 1400 rpm for 10 minutes at 4°C followed by washing thrice by sterile phosphate buffered saline (PBS, pH 7.4). These cells were further incubated at 37°C for 3 hours after replacement of the previous media by fresh 0.5 $mg.ml^{-1}$ of MTT reagent containing media. After this incubation, cells were again incubated at room temperature (27^0C) for 15 minutes after adding isopropanol-HCL solution. Spectrophotometer was used to measure the absorbance of formed formazan-MTT product in a Shimadzu UV–Vis 2600 spectrophotometer at 570 nm [51].

8. Determination of bacterial intracellular ROS generation

2,7-dichlorofluorescein di-acetate (DCF-DA) mediated protocol [52] was implemented to measure reactive oxygen species (ROS) generation within bacterial cells. 2, 7-dichlorofluorescein (DCF), which is a highly fluorescent compound, is generated as a result of reaction between ROS generated within the bacterial cells and passively entered DCF-DA into the cells. The bacterial cells were incubated overnight with both synthesized and commercial ZnONPs and subjected to wash with phosphate buffer solution on the next day, followed by addition of needed amount of DCF-DA. After incubating the bacterial cells for half an hour at 37^0C, results were obtained spectroscopically [53].

9. Bacterial SEM study

The extent of physical interaction of both the green synthesized and commercial ZnONPs with the treated bacterial cells, followed by damage of bacterial cell morphology was analyzed by scanning electron microscopy (SEM) study. Samples were prepared following previously reported method [54]. Centrifugation (4 min, 4000 RPM) of 6 hours incubated 1 ml treated bacterial cells along with control was performed to acquire the pellet. Filtered sterile PBS containing 2% glutaraldehyde was utilized to wash the pellets thrice and then subjected to dehydration using serially diluted ethanol. D r o p casting of the cells were then performed on cover slips and kept under laminar air flow for drying. Samples were further gold coated after placing on carbon tape for bacterial SEM analysis (FEI, INSPECT F50, Netherlands).

10. Synergistic study

For evaluating the synergistic effect of combination of resistant antibiotic (ampicillin) with both the ZnONPs (Commercial and Green), checker board titration method [55] was used (Climo et al., 1999). The combinations of ZnONPs and ampicillin were made by adding them in concentrations lower than their individual MIC values in a 96 well plate by serial dilution. Similar process was followed in case of both types of ZnONPs. Each well was inoculated with bacterial culture containing approximately 1.5 x 10^8 CFU.mL^{-1} cells and incubated at 37°C for 24 hours and the MIC values were determined by identifying the well having no turbidity. To evaluate whether the combinations of above-mentioned nanoparticles with ampicillin have synergistic effects or not, the Fractional Inhibitory Concentration Index (FIC Index) was calculated by using the formula:

For commercial ZnONPs: ΣFIC= FIC C + FIC A, where FIC C = (MIC of agent C in combination)/ (MIC of agent C); FIC A = (MIC of agent A in combination)/ (MIC of agent A).

For green synthesized ZnONPs: ΣFIC= FIC G + FIC A, where FIC C = (MIC of agent G in combination)/ (MIC of agent G); FIC A = (MIC of agent A in combination)/ (MIC of agent A)

The result is considered synergistic when ΣFIC index is ≤0.5, indifference ΣFIC index >0.5 to ≤ 4 and antagonistic ΣFIC index >4.

E. MULTIPLE ANTIBIOTIC RESISTANT *S. aureus* INDUCED DEVELOPMENT OF INFLAMMATORY RAT MODEL

1. *S. aureus* induced inflammatory rat model

For the development of inflammatory model (*in vivo*), 48 white male rats (Wistar strain) weighing between 130 – 150 gm were used. These animals were maintained at standard laboratory conditions (14 hours light: 10 hours dark, 25 ± 2°C temperature) for 10 days with free access to food and water. The standard laboratory diet was composed of 71% carbohydrate, 18% protein [consisting of whole wheat flour (3.62%), roasted Bengal gram flour (4.38%) and casein

(10%)], 7% fat, 4% salt mixture and vitamins [56]. Animals were divided into 8 groups with 6 animals placed in each group. Treatments administered intraperitonially to all the animals are presented in the following table. The experiments were performed following the guidelines implemented by the Committee for the Purpose of Control and Supervision of Experiments on Animals, India, with approval from the Animal Ethics Committee of Presidency University (Sanction number: PU/IAEC/MS/19).

GROUP-1	Control: Injected with sterile saline.
GROUP-2	Infected: By fresh culture (optical density = 0.4) of *S. aureus* (KC 02) for development of inflammation.
GROUP-3	Treated: By ZnONPs (green synthesized).
GROUP-4	Treated: By ZnONPs (commercially available).
GROUP-5	Infected and Treated: By green synthesized zinc oxide nano particles after inflammation development.
GROUP-6	Infected and Treated: By commercial zinc oxide nano particles after inflammation development.
GROUP-7	Infected and Treatment by the combination (green synthesized zinc oxide nano particles and antibiotic) after inflammation development.
GROUP-8	Infected and Treatment by the combination (commercial zinc oxide nano particles and antibiotic) after inflammation development.

Table 1: Distribution of animals in different groups to perform proposed in vivo study.

Inflammation development and Treatment Plan								
GROUPS	DAY 0	DAY 1	DAY 2	DAY 3	DAY 4	DAY 5	DAY 6	DAY 7
1	0.2 ml (0.9% NaCl)	-	-	-	-	-	-	Sacrifice
2	0.2 ml (KC 02)	-	-	Sacrifice (3 animals)	-	-	-	Sacrifice (3 animals)
3	-	-	-	0.2 ml (Green=28µg/ml)	0.2 ml (Green=28µg/ml)	0.2 ml (Green=28µg/ml)	0.2 ml (Green=28µg/ml)	Sacrifice
4	-	-	-	0.2 ml (Commercial=34.6µg/ml)	0.2 ml (Commercial=34.6µg/ml)	0.2 ml (Commercial=34.6µg/ml)	0.2ml (Commercial=34.6µg/ml)	Sacrifice
5	0.2 ml (KC 02)	-	-	0.2 ml (Green=28µg/ml)	0.2 ml (Green=28µg/ml)	0.2 ml (Green=28µg/ml)	0.2 ml (Green=28µg/ml)	Sacrifice
6	0.2 ml (KC 02)	-	-	0.2 ml (Commercial=34.6µg/ml)	0.2 ml (Commercial=34.6µg/ml)	0.2 ml (Commercial=34.6µg/ml)	0.2 ml (Commercial=34.6µg/ml)	Sacrifice
7	0.2 ml (KC 02)	-	-	0.2 ml (ZnONPs=1.8 µg/ml; Antibiotic=8.2 µg/ml)	0.2 ml (ZnONPs=1.8 µg/ml; Antibiotic=8.2 µg/ml)	0.2 ml (ZnONPs=1.8 µg/ml; Antibiotic=8.2 µg/ml)	0.2 ml (ZnONPs=1.8 µg/ml; Antibiotic=8.2 µg/ml)	Sacrifice
8	0.2 ml (KC 02)	-	-	0.2 ml (ZnONPs=2.3 µg/ml; Antibiotic=9.6 µg/ml)	0.2 ml (ZnONPs=2.3 µg/ml; Antibiotic=9.6 µg/ml)	0.2 ml (ZnONPs=2.3 µg/ml; Antibiotic=9.6 µg/ml)	0.2 ml (ZnONPs=2.3 µg/ml; Antibiotic=9.6 µg/ml)	Sacrifice

Table 2: Group-wise inflammation development and treatment plan. Group 1=Control, Group 2= Treated with *S. aureus* only, Group 3= Treated with only green synthesized ZnONPs, Group 4= Treated with only commercial ZnONPs, Group 5= Treated with only green ZnONPs after inflammation development, Group 6= Treated with only commercial ZnONPs after inflammation development, Group 7= Treated with combination (antibiotic + green ZnONPs) after inflammation development, Group 8= Treated with combination (antibiotic + commercial ZnONPs) after inflammation development.

F. STUDY OF THE ANTIMICROBIAL AND ANTI-INFLAMMATORY EFFECT OF ZnONPs ON THE INFLAMMATION MODEL

1. Signs of inflammation development

Circumference of the knee joints for the animals of all groups were measured pre and post exposure to treatment agents on respective intervals starting from day 0 (zero). A flexible tape [57, 58] was wrapped around the joint to obtain the measurements. These values of the knee circumference were used to compare the effect of inflammation, followed by the treatment, with the normal value.

Changes associated to footpad was also noticed before and after inflammation and treatment for the animals of group 2 to 8.

2. Collection of joint fluid

On day 3 and 7, fluid from the knee joints from animals of all groups, was collected using 0.9% saline. This fluid was then cultured on blood agar plates [59] followed by overnight incubation at 37^0C. The bacterial colonies growing on the culture plates were counted to determine bacterial load in response to the anti-inflammatory agents.

3. Blood Collection

DAY 03 – Blood was aseptically collected from tail vein [60] of all animals.

DAY 07 - Rats (group 1 to 8) were anesthetized by anesthetic ether before being subjected to cardiac puncture. Sterile condition was maintained during blood collection. Sample was distributed in two parts, one kept in ethylenediaminetetraacetic acid (EDTA) and the other was placed in heparinized containers [61].

4. Erythrocyte and Leucocyte Count

A portion of whole blood was diluted (1:200) using physiologic saline (0.9% NaCl) before loading 15 to 20 µl of the suspension into the hemocytometer. RBCs were then counted after adjusting the magnification of the microscope at 40X [62].

Cells/µl = Number of cells counted × Dilution factor × 5 / Volume factor.

For measuring WBC count, a part of whole blood collected (Group 1 to 8) was diluted in saline (1:20). A small amount of the diluted blood was loaded in hemocytometer and counting of cells were performed under compound microscope (10X). The obtained results were used to calculate the total number of leucocytes according to the following expression [63].

Cells/µl = Number of cells in 1 large square × Dilution factor / Volume factor.

5. Assay of Erythrocytes

- **Osmotic fragility Test –** Heparinized blood (group 1 to 8) was placed in a set of tubes containing 0.0, 0.1, 0.3, 0.5, 0.7, 0.9 g/L of NaCl (pH 7.4). These tubes were then incubated at room temperature (27^0C) for 30 min. Next, the tubes were subjected to centrifugation at 800g for 10 min. The supernatant of all the tubes were collected in glass cuvette and used for measuring the optical density at 540 nm. The collected data of spectroscopic measurement was utilized to determine percentage erythrocyte hemolysis by using the following formula:
  % hemolysis = Optical density of test solution /Optical density of standard solution ×100 [64]
- **Malondialdehyde concentration determination –** Briefly, erythrocytes (group 1 to 8) were isolated from heparinized blood using centrifugation technique. These isolated erythrocytes were washed with cold saline (isotonic) and used along with thiobarbituric acid (TBA) to determine malondialdehyde (MDA) concentration spectroscopically at 532 nm [65].

6. Serum isolation

After collection, blood was taken in vials, free from anticoagulant and kept still for 30 min at room temperature. These samples were then centrifuged at 3500 rpm for 20 min [66]. The supernatant was collected as serum and further used for biochemical assays.

7. Enzymatic assay

Serum collected from the animals on both day 3 and 7 was used to identify hepatic function. Serum glutamate oxaloacetate transaminase (SGOT) and serum glutamate pyruvate transaminase (SGPT) were assayed [67] three times from each sample using standard protocol (Span diagnostics Ltd.).

8. Study of inflammatory markers

Sandwich ELISA was used to identify the changes in level of both pro-inflammatory [68] and (IL-6,8, TNFα, C-reactive protein) anti-inflammatory [69] (IL-10) cytokines. The assay was performed from serum sample, isolated from whole blood of animals (Group 1 to 8), as per the instructions provided with the kits (Thermo Fisher). Finally, after completing incubation, absorbance of the prepared samples was measured at 450 nm by ELISA reader (Bio-Rad Model 680). The results were obtained using standard curves for each marker.

9. Study of cytokine modulator

Beside pro-inflammatory and anti-inflammatory markers, serum level of histamine (for all group animals), a cytokine modulator was also studied using standard protocol for competitive ELISA (enzyme-linked immunosorbent assay), instructed in the kit (Abcam213975). After incubation and absorbance measurement at 450 nm, histamine levels were determined using standard curve [70].

10. Histology

Collected tissues (spleen, liver, kidney, adrenal gland) were fixed using buffered formol before embedding in paraffin. Routine hematoxylin/eosin (H/E) staining was performed using tissue sections of 5µ thick, prepared by a high precision microtome (Model IEC Microtome, USA). These tissue sections were observed under microscope (100X magnification) [71].

11. Statistical Analysis

Each experiment was repeated in triplicate. Standardization of data was done using one-way ANOVA and two-tailed t-test. Significant differences were compared using $P<0.05$ level of significance in Microsoft Excel.

V. Results

Objective 1: Characterization of ZnONPs with respect to their size, mass, etc.

XRD analysis: X-ray diffraction study (Figure:1) of both green synthesized and commercial ZnONPs revealed nice crystalline structure having evident diffraction peaks and also portrayed the influence of circumstantial conditions maintained throughout the synthesis procedure of green ZnONPs. At 2θ values 31.81, 34.59, 36.36, 47.62, 56.71, 63.03, 66.57, 68.09, 69.22 and 32.02, 34.68, 36.44, 47.65, 56.80, 63.14, 66.67, 68.15, 69.47 distinct characteristic peaks were observed for green and commercial ZnONPs respectively, corresponding to (hkl) values of (100), (002), (101), (102), (110), (103), (200), (112), (201). The hexagonal Wurtzite ZnONPs structure approved by Joint Committee on Powder Diffraction Studies Standards (JCPDS card number 008, 82-1042 and 5-0664) resembles with the observed plane values. Inexistence of any additional peak confirms the formation of pure sample. Equation of Debye–Scherer was applied to calculate average size of both the green and commercial ZnONPs utilizing the highest peak. The size of both the ZnONPs evaluated from this study confirms its nano-scale structure [34]. $D=0.9\lambda/\beta \cos\theta$ [λ = wavelength (1.5418 Å), θ = Bragg's diffraction angle, β = full width at half maximum]

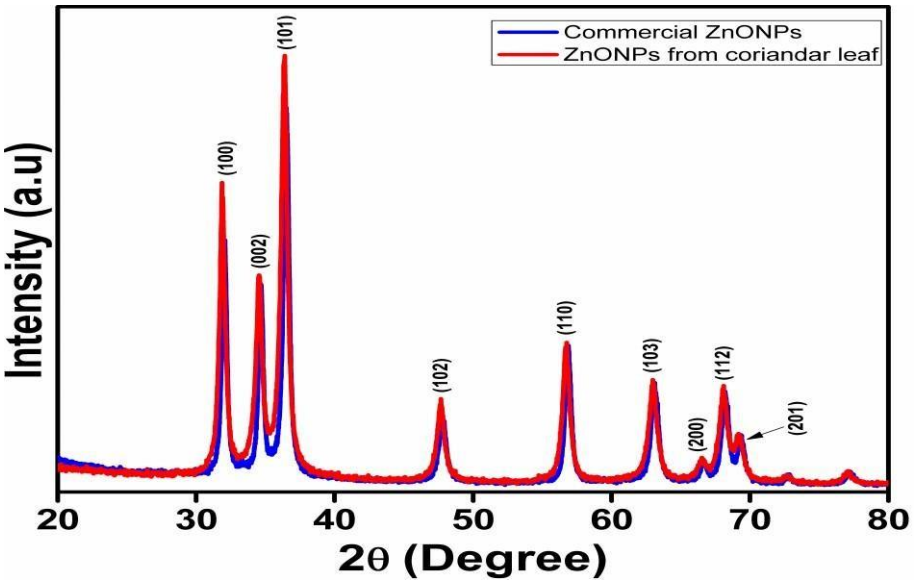

Figure 1 Size determination of ZnONPs (Outsourced from Department of Physics, Jadavpur University, Kolkata)

Spectroscopic Analysis: Purity of both the green synthesized and commercial ZnONPs were investigated through FTIR analysis (Figure:2). Absorption band of both the ZnONPs were

observed within a range of 4000-500 cm^{-1}. Peak at around 450 cm^{-1} confirms the existence of M-O and ZnO vibrational band as this peak demonstrate, ZnO bond stretching frequency. Peak at 774 cm^{-1} accounts for the intra-molecular hydrogen bond's –OH stretching along with C=O and C-C stretching of alkanes. Peak at around 1104 cm^{-1} can be the contribution of N-C stretching vibration of aromatic and aliphatic amides, aliphatic amines, phenolic and alcohol groups along with secondary amines stretching vibration. Existence of atmospheric CO_2 and amide linkage within amino acid residues are expressed by band at 3376 cm^{-1}[145] [35].

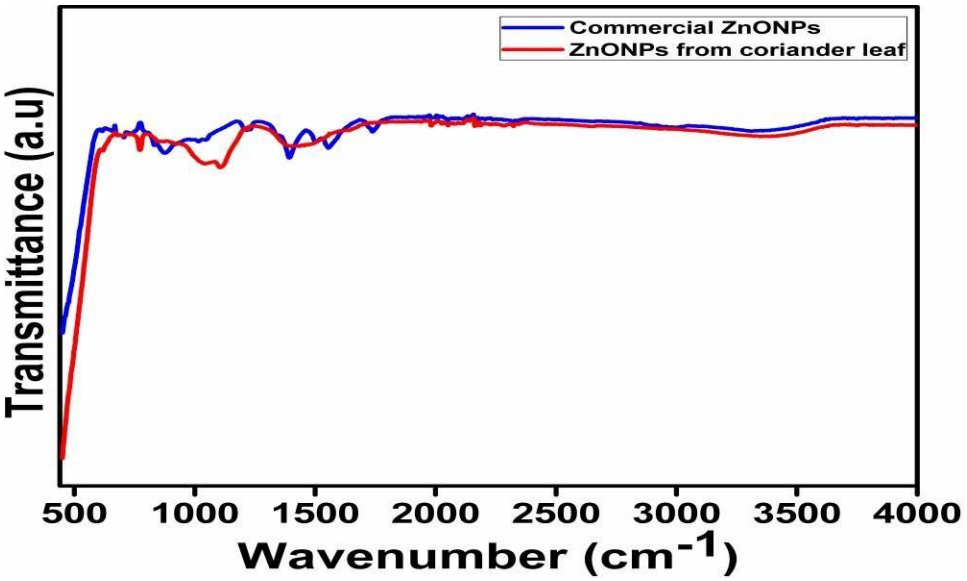

Figure 2 Purity determination of ZnONPs (Outsourced from Department of Physics, Jadavpur University, Kolkata)

Determination of hydrodynamic size and surface charge of ZnONPs: Dynamic Light Scattering (DLS) analysis was conducted to evaluate the average size of both commercial and green synthesized ZnONPs along with their Zeta potential. Table:3 represents the observed average diameter and Polydispersive index (P.D.I) of both the ZnONPs which are in accordance with literature [36]. As shown in the table below, zeta potential of green synthesized ZnONPs is more than that of the commercial one. This result depicts, the biogenic nanoparticles are more stable in aqueous medium which in turn is quite conducive for biological applications.

SAMPLE NAME	DLS SIZE(d.nm)	Polydispersive index	ZETA POTENTIAL (mV)
ZnONPs From coriander leaves	87.6±2.7	0.143	13.34±2.7

Commercial ZnONPs	85.6±2.2	0.152	11.45±1.8

Table 3: Representing stability profile of both ZnONPs (Outsourced from Department of Physics, Jadavpur University, Kolkata)

FE-SEM analysis: The structural evaluation of both the green and commercial ZnONPs were conducted through FE-SEM study (Figure:3). Resultant micrograph images display spherical shape along with identical ordination for both green synthesized and chemically synthesized commercial ZnONPs. The morphology of green synthesized ZnONPs is in accordance with other reported green nanoparticles [37]. This satisfactory result of FE-SEM study further confirms that, there was no morphological variation between green synthesized and commercial ZnONPs.

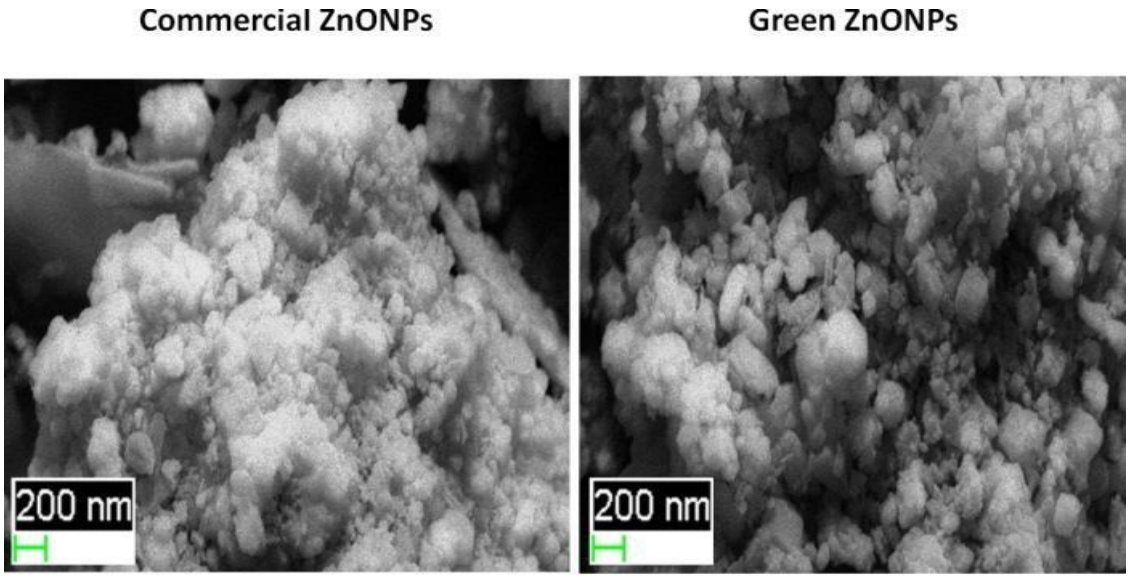

Figure 3 Morphology determination of ZnONPs (Outsourced from Department of Physics, Jadavpur University, Kolkata)

Result of bacterial strain identification

The images obtained after performing Gram staining (Figure:4) indicates the presence of Gram-positive strains of bacteria in the test sample.

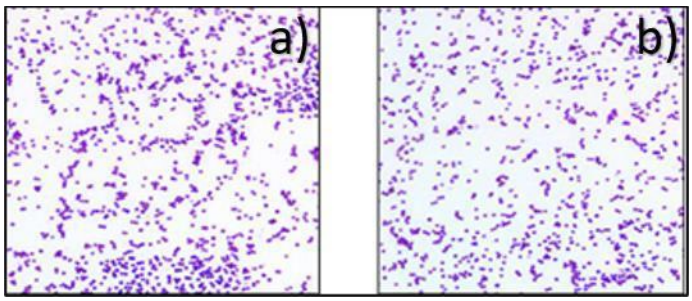

Figure 4: Gram-staining of bacterial strains a) ATCC25923 and b) KC-02. Presence of only Violet colour in the image confirms both strains are Gram Positive.

Results obtained after performing the Catalase test. Both the control and clinical strain (KC-02) gave positive catalase test (Figure:5).

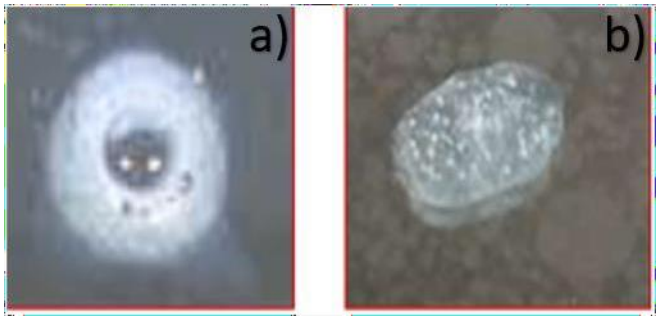

Figure 5: Both the strains a) ATCC25923 and b) KC-02 of *S. aureus* produce enzyme catalase, resulting in breaking down hydrogen peroxide to form water and oxygen.

Nucleotide Sequence Accession Number

The clinical strain (KC-02) subjected to molecular identification proved to be a strain of *S. aureus* with Gene Bank Accession Number- MW221984 (Certificate Attached)

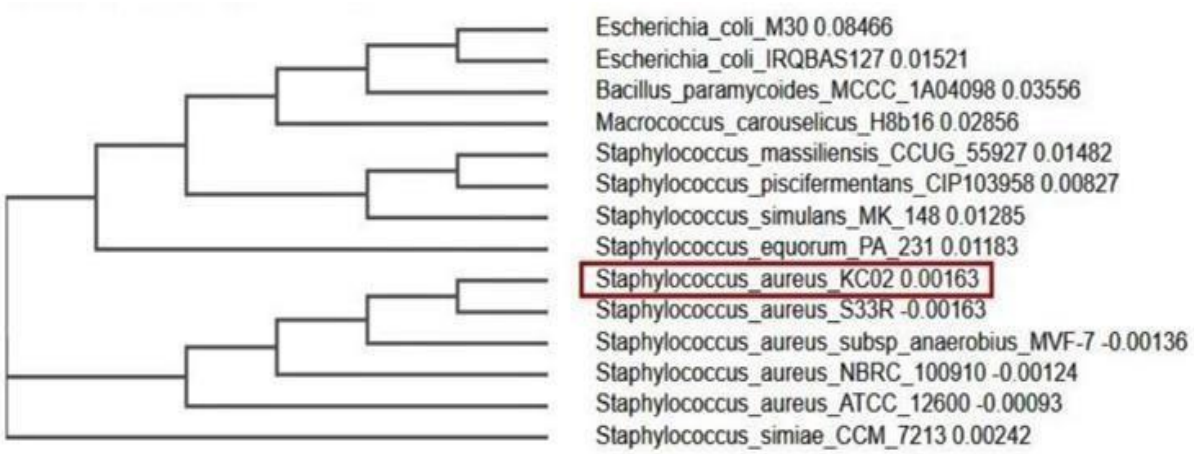

Figure 6: To identify the microbe of interest isolated from clinical source, phylogenetic tree was generated using the Clustal Omega multiple sequence alignment algorithm by applying neighbor joining method based on 16S rDNA sequences. 15 different nucleotide sequences with maximum identity were used for analysis, higher query coverage and lower distance matrix (as per Kimura-2-Parameter model) with the newly obtained 16S rRNA sequence.

Result of Disk diffusion Test

ANTIBIOTICS	ATCC25923	KC-02 (Clinical)
	Zone of Inhibition (mm)	
1. Ampicillin (10µg)	30	20
2. Amikacin (30µg)	20	13
3.Cefexime (5µg)	19	12
4.Chloramphenicol (30µg)	16	11
5.Tetracycline (30µg)	22	16

Table 4: Representing antibiotic susceptibility of both control and clinical strain of *S. aureus*

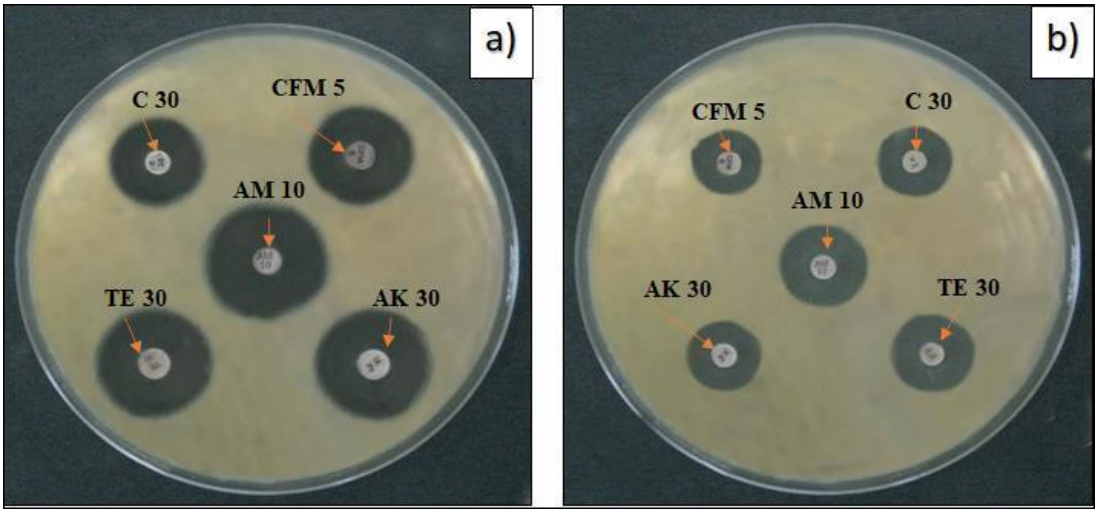

Figure 7: Result of antibiotic susceptibility test by DAD of both strains of *S. aureus* a) ATCC25923 and b) KC-02. C= Chloramphenicol, **CFM=** Cefexime, **AM=** Ampicillin, **TE=** Tetracycline and **AK=** Amikacin.

The control strain was sensitive to the above antibiotics and the test strain was resistant to all the above antibiotics, as per CLSI guidelines.

Comparative analysis of antibacterial efficacy between green and commercial ZnONPs

Antibacterial effectiveness of both the green synthesized and commercial ZnONPs were investigated against both strains of *S. aureus* (ATCC25923 and KC-02). Obtained MIC values for each specific strain enlisted in table below. Each bacterial strain was cultured in sterile Mueller Hinton agar plate containing the obtained MIC dilution. MBC was considered to be the dose of ZnONPs at which there is complete killing of bacteria without any further growth. Values in the given table state the MBC values for both the bacterial strains used. It can be easily concluded that, the MIC and MBC values for green ZnONPs is significantly lower ($p<0.05$) than commercial one for each bacterial strains used.

Concentrations	**Bacterial strains**	
	ATCC25923	KC-02
	Green synthesized Zinc Oxide Nano-particles	
MIC (µg/ml)	26.8±1.3	28.0±2.1
MBC (µg/ml)	102.8 ± 1.8	104.3 ± 2.4
	Commercial Zinc Oxide Nano-particles	

MIC (µg/ml)	30.3±2.8	34.6±2.3
MBC (µg/ml)	108.8 ± 2.1	110.4 ± 1.9

Table 5: MIC and MBC values of both ZnONPs against strains of *S. aureus*. The data are the average of three experiments ± SD.

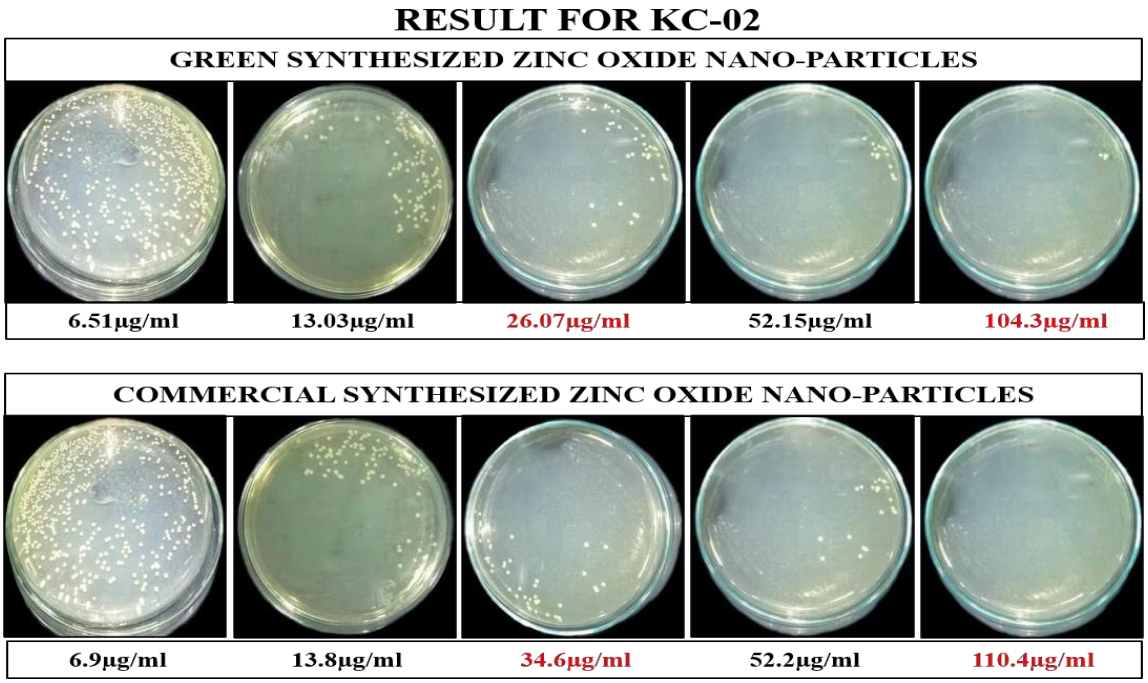

Figure 8: Determination of MBC of synthesized green and commercially available ZnONPs by spread-plate technique against KC-02 strain of *S. aureus*

Comparison between the effective bactericidal activity of green and commercial ZnONPs

Tolerance level is a tool of discrimination between bactericidal and bacteriostatic agents. MBC and MIC value for any bacterial strain equipped the identification of this level. Reversible bacterial growth inhibition occurs by bacteriostatic agents whereas, non-reversible total destruction of bacterial growth occurs by bactericidal one. Agents are said to be bacteriostatic when the MBC/MIC ratio is more than or equal to 16 and bactericidal when the ratio is less than or equal to 04. In this study, the ratios for strains of *S. aureus* (ATCC25923 and KC-02) were less than 04, after treating the strains with commercial and green ZnONPs separately.

Confirmation study of bactericidal activity

Treatment of both bacterial strains of *S. aureus* (ATCC25923 and KC-02) with their respective MBC values of green synthesized and commercial ZnONPs, gave rise to clear zones of inhibition after performing Agar well diffusion study (Figure:9). After comparing the obtained zones of inhibition with that of the positive control (sensitive antibiotic used- Doxycycline), it was found that, bactericidal effect exhibited by used antibiotic, commercial and green synthesized ZnONPs was almost same for their respective MBC values against the test organisms.

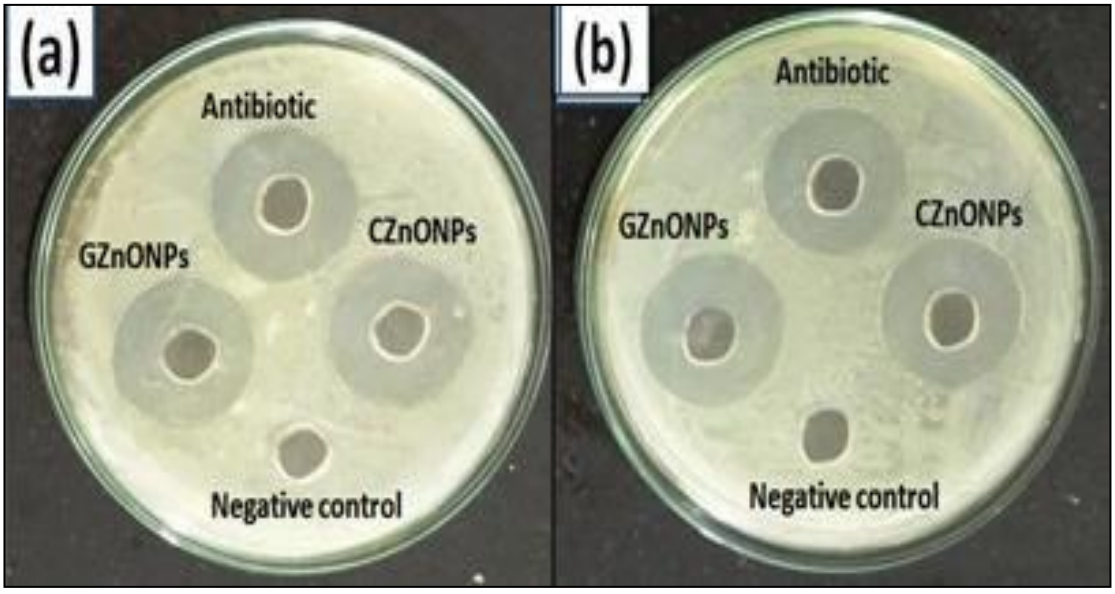

Figure 9 Confirmation of MBC values for both ZnONPs against (a) ATCC25923 and (b)KC-02 strains of *S. aureus*

Bacterial growth inhibition dynamics

Bacterial growth pattern (Figure:10) as observed for each strain of *S. aureus* (ATCC25923 and KC-02) after plotting the curves indicates, relation between growth inhibition and time. The interpretation of the plotted graph also reveals significantly higher ($p<0.05$) inhibition potential of green ZnONPs compared to commercial one.

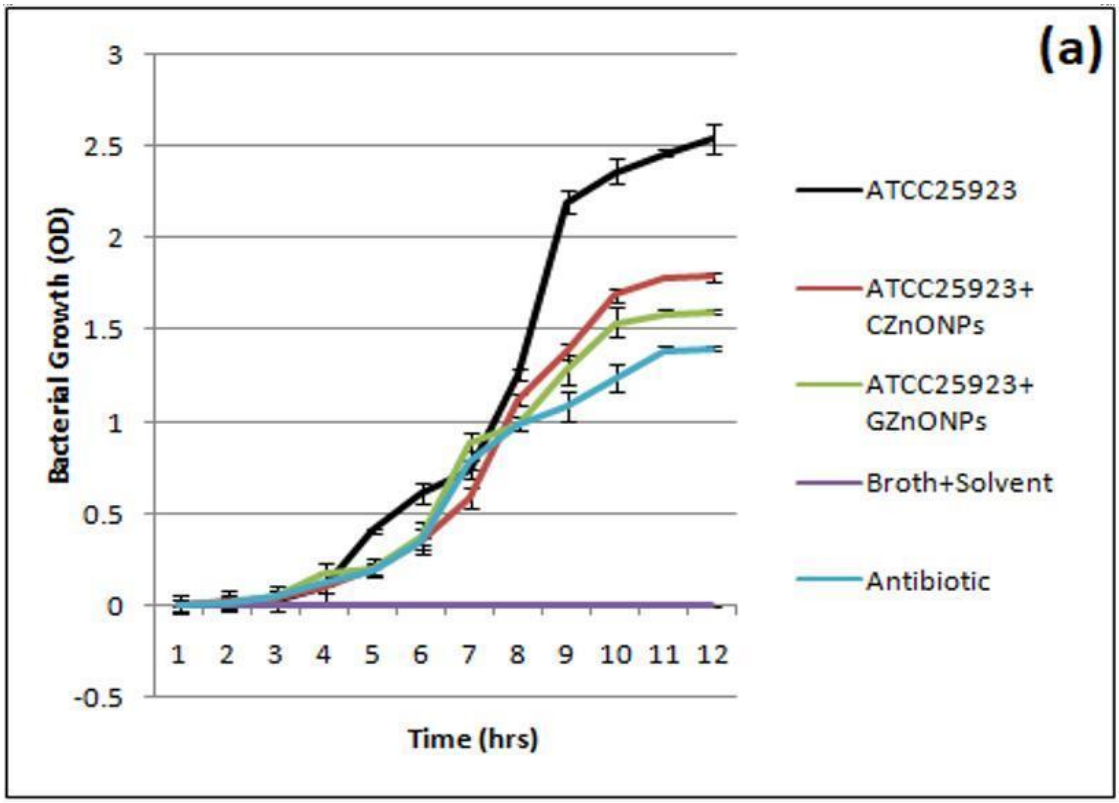
(a)
Bacterial Growth (OD)
Time (hrs)
ATCC25923
ATCC25923+ CZnONPs
ATCC25923+ GZnONPs
Broth+Solvent
Antibiotic

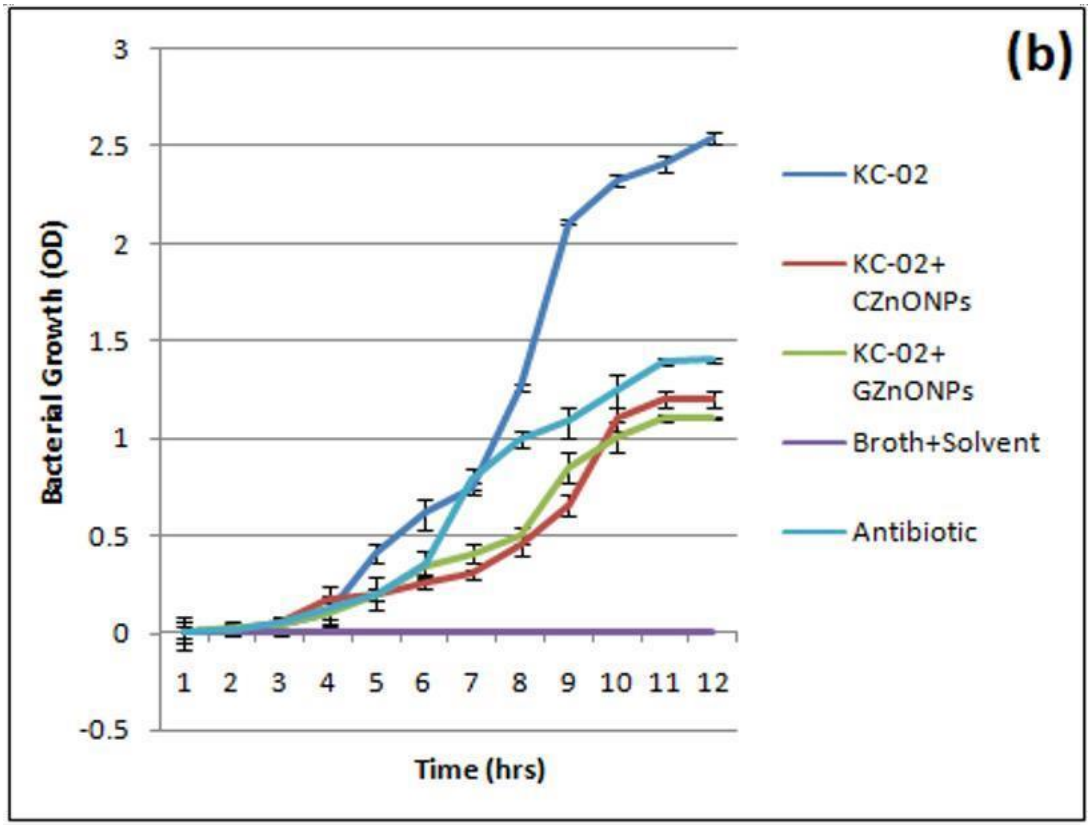
(b)
Bacterial Growth (OD)
Time (hrs)
KC-02
KC-02+ CZnONPs
KC-02+ GZnONPs
Broth+Solvent
Antibiotic

Figure 10 Growth inhibition dynamics for both ZnONPs (a) ATCC25923 and (b) KC-02 strains of *S. aureus.* The data are the average of three experiments ± SD.

ZnONPs significantly reduces the viability of bacterial cells

Figure:11 illustrates the result of MTT assay which was performed to determine bacterial cell viability in response to both green and commercial ZnONPs. It was clearly observed that, viability of bacterial cells notably diminished at their corresponding MBC dose for both green synthesized and commercial ZnONPs. Statistically significant ($p<0.05$) differences were observed between green synthesized and commercial ZnONPs in relation to their inhibition potential in case of both the strains of *S. aureus* (ATCC25923 and KC-02). Penetration of ZnONPs inside the treated bacterial cells followed by cessation of cell growth may account for the bactericidal activity of ZnONPs [51].

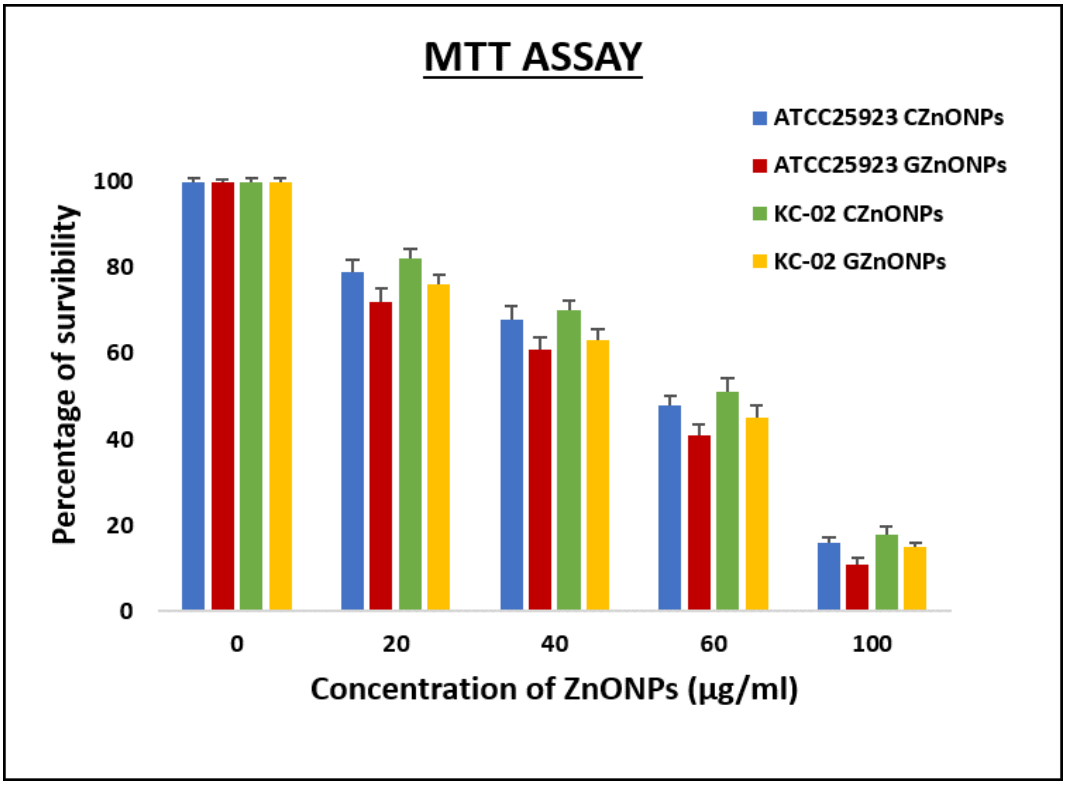

Figure 11: Bacterial cell viability response to commercial and green synthesized ZnONPs. The data are the average of three experiments ± SD.

Probable mechanism of action justifying the bactericidal activity of ZnONPs:

Both the green synthesized and commercial ZnONPs potentially uplift intracellular ROS formation which renders the cells under apoptosis. In an attempt to reveal the mechanism of action underlying the bactericidal efficacy of ZnONPs, ROS generation inside the treated bacterial cells were measured by administrating an indicator of intracellular ROS formation, DCF-DA (Figure:12). Both the green and commercial ZnONPs proved to be responsible for augmentation of ROS generation inside the treated bacterial cells, leading to cell death. Significant difference in intracellular ROS generation ($p<0.05$) by green and commercial ZnONPs was clearly observed in this study. Generation of intracellular ROS and cell death shares a linear relationship as increased generation of intracellular ROS leads to enhancement in cell death as an obvious fate of damaged cell membrane, respiratory chain disruption and destruction of genetic material [53].

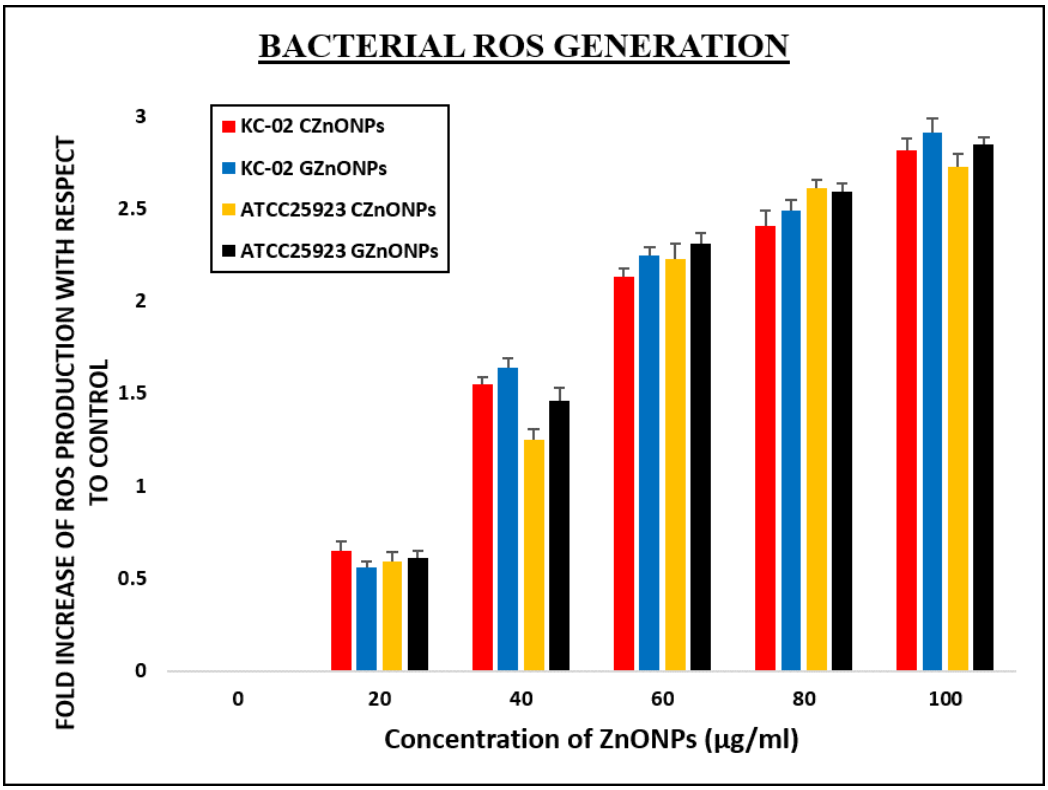

Figure 12: Effect of commercial and green synthesized ZnONPs in bacterial ROS generation. The data are the average of three experiments ± SD.

Effect on bacterial morphology

Membrane destruction of bacterial cells occurred under influence of treatment by both green and commercial ZnONPs, revealed through SEM images (Figure:13). Possible penetration of ZnONPs was the underlying cause for membrane leakage resulting in expulsion of cytoplasmic material. This was followed by clumping of bacterial cells post treatment by ZnONPs. A slightly higher antibacterial effect was executed by green ZnONPs in comparison to commercial one, as observed in the SEM images. As a whole, treating bacterial cells by both green and commercial ZnONPs lead to loss of its morphological integrity followed by death of the microorganism.

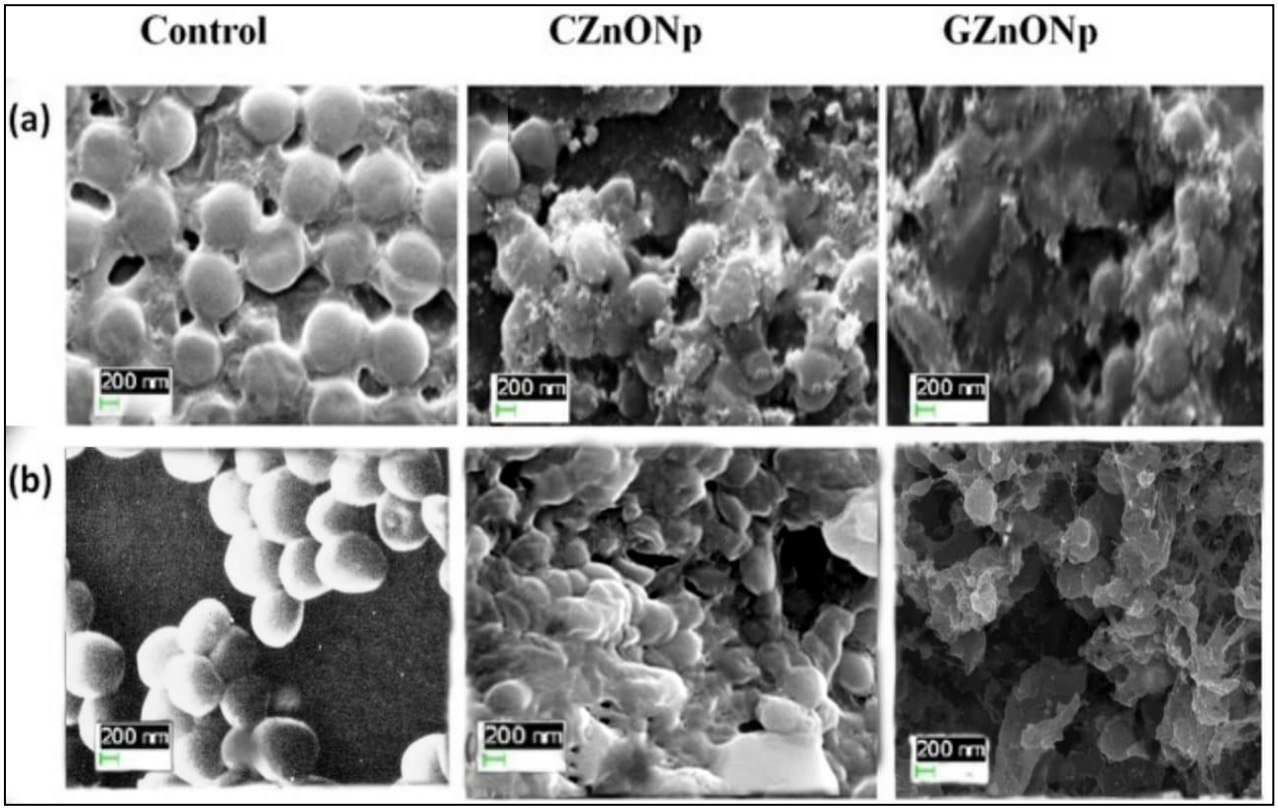

Figure 13: SEM images of the effect of commercially available and green synthesized ZnONPs on (a) ATCC25923 and (b) KC-02 strains of *S. aureus* (Outsourced from Department of Physics, Jadavpur University, Kolkata)

Synergistic Effect:

Serial No.	Strains of *S. aureus*	Commercial ZnONPs (C) MIC	Green ZnONPs (G) MIC	Ampicillin (A) MIC ($\mu g\ mL^{-1}$)	Combined (C/A) MIC	Combined (G/A) MIC	FIC Index (C-	FIC Index (G-	Result of action

		($\mu g\ mL^{-1}$)	($\mu g\ mL^{-1}$)		($\mu g\ mL^{-1}$)	($\mu g\ mL^{-1}$)	A)	A)	
1.	ATCC-25923	30.3±2.8	26.8±1.3	16.4±1.5	2.02/2.9	1.7/1.09	0.23	0.12	Synergistic
2.	KC-02	34.6±2.3	28.0±2.1	123.5±1.7	2.3/9.6	1.8/8.2	0.13	0.12	Synergistic

Table 6: Representation of the combined antibacterial effect of both ZnONPs with antibiotic against strains of *S. aureus*. The data are the average of three experiments ± SD. Significant difference ($p<0.05$) was observed in FIC index determined for both ZnONPs in case of ATCC25923 strain but no such difference ($p>0.05$) can be reported in case of KC-02 strain of *S. aureus.*

The result clearly indicates synergistic action of the combination [55] of nanoparticle with antibiotic at much lower concentrations then the MIC values of the individual antibacterial agents.

Objective2: Multiple antibiotic resistant *S. aureus* induced development of inflammatory rat model

Inflamed knee joint and footpad

The knee circumference of control group measured 55.2 ± 0.3 mm (n=6) whereas, that of group 2,5,6,7 and 8 gave a measure of 70.5 ± 0.4 mm (n=6) circumference on day 3. This indicates a prominent development of knee joint inflammation. Group 3 and 4 showed no such changes in knee circumference. Group 5 to 8 gave almost normal values ($p>0.05$) with respect to group 1 results of knee circumference, when measured on day 7, indicating recovery from inflammation.

After day 3, footpad swelling [58] for animals of group 2, 5 to 8 was observed, supporting the development of hindlimb inflammation (Figure:14). At the end of treatment with respective anti-inflammatory agents, swelling of footpad successfully disappeared.

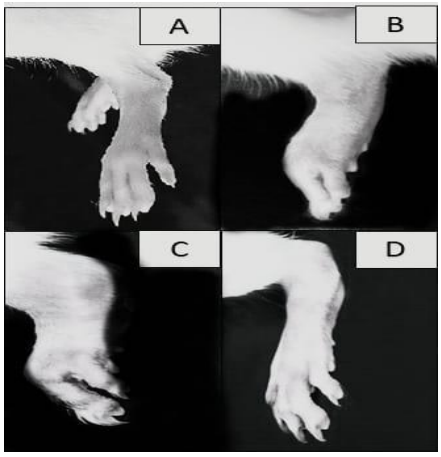

Figure 14: Representative images of rat-paw from *S. aureus* induced inflammation model-(Development and treatment); (A) Group-1, (B) Group-2, (C) Group-5 Day 03 and (D) Group-5 Day 07.

Evaluation of Colony count

The colony count result clearly indicates, observable amount of bacterial load reduction (Figure:15) on exposure to treatment by respective agents. No statistically significant difference was observed ($p>0.05$) when group 1 day 07 result was compared with result of rest of the groups excluding group 2.

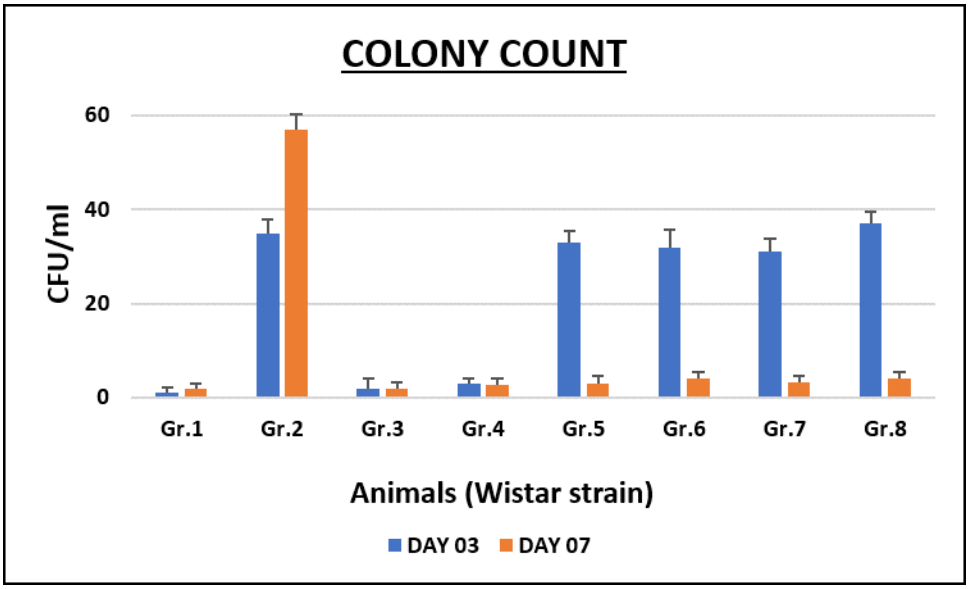

Figure 15 Determination of bacterial load by colony count method. The data are the average of three experiments ± SD.

Objective 3: Study of the antimicrobial and anti-inflammatory effect of ZnONPs on the inflammation model

Results of Erythrocyte and Leucocyte Count

The count of erythrocytes showed (Figure:16) no variation among the animals of different groups ($p>0.05$). These holds correct, both on day 3 and 7. The RBC count of control group and the other groups (2 to 8) were in the range of 8.02 to 8.04 ± 0.1 ($10^3/\mu l$) [31].

On day 3, group 2 and 5 to 8 showed significant rise in the WBC count (Figure:17). Group 1, 3 and 4 showed normal level WBC count. As per the WBC count on day 7, group 2 (untreated) gave further rise in leucocyte count whereas, the animals of treated groups (5 to 8), gave almost normal leucocyte count ($p>0.05$) as compared to the control group [63].

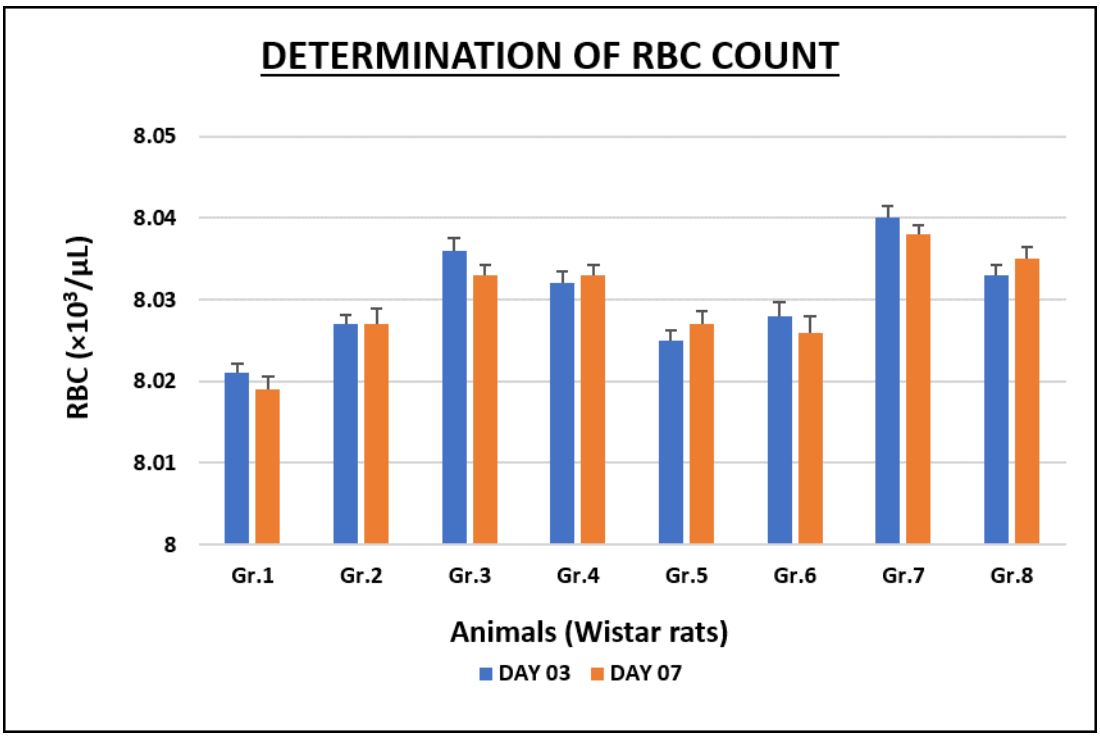

Figure 16 Comparison of RBC count. The data are the average of three experiments ± SD.

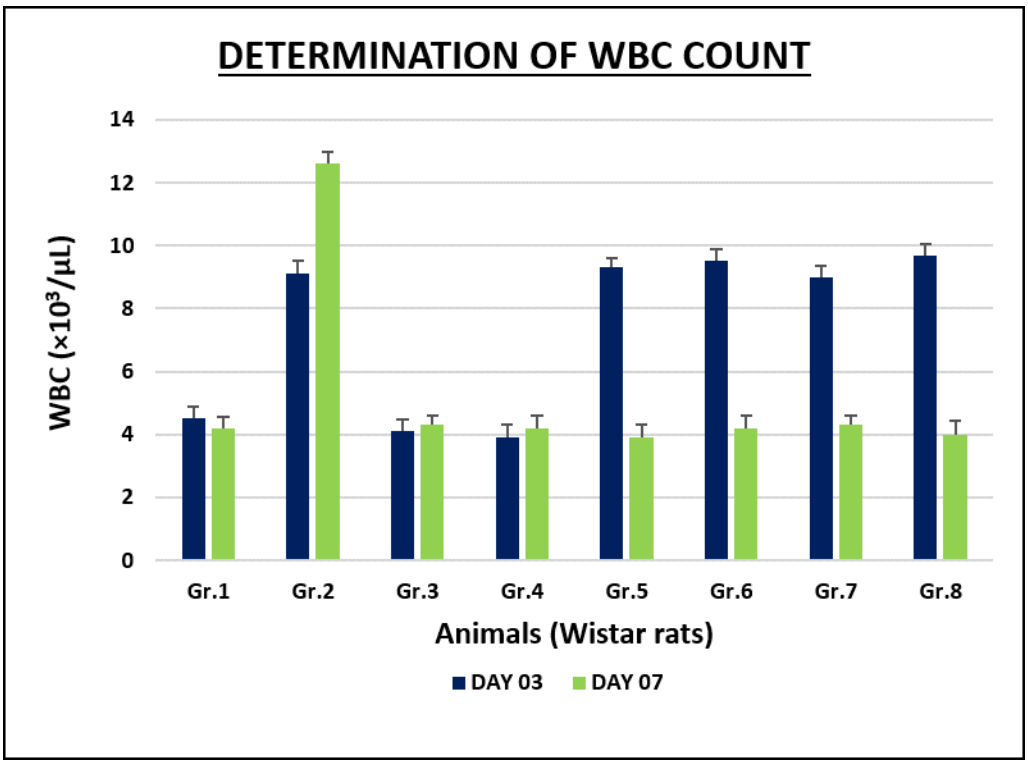

Figure 17: Comparison of WBC count. The data are the average of three experiments ± SD.

Results of osmotic fragility test

Maximum fragility (100%) of erythrocytes (group 1 to 8) occurred when exposed to 0.0 g/L of NaCl. Percent fragility decreased with gradual increase in NaCl concentration. Almost intact erythrocyte membranes were available for all groups at 0.9 g/L NaCl [64].

Results of MDA concentration determination

MDA concentration for all group animals were in the range of 105 to 115 mmol/g hemoglobin. This clearly indicates, the erythrocytes of animals (both control and exposed to anti-inflammatory agents) did not suffer from lipid peroxidation [65].

Result of Enzymatic assay

Results clearly indicate, no deviation of these hepatic enzymes occurred in both group 3 and 4, administered with ZnONPs (Green and commercial) only, till 7^{th} day. In case of the treated

groups, both the assayed enzymes were in normal range (SGOT=68.3±4.2 U/L; SGPT=121±3.8 U/L) [67] when observed on day 3 and 7. This clearly indicate, used concentrations of ZnONPs (alone and in combination with antibiotic) were unable to generate significant ($p>0.05$) measurable amount of oxidative stress.

Result of inflammatory marker assay

The increased serum level of inflammatory markers, as shown by figures 18 and 19, clearly indicates expected *S. aureus* induced inflammatory response at the end of day 3. The levels of the markers at the end of day 7, shows prominent decrease of inflammatory response due to treatment by selected anti-inflammatory agents. No statistically significant difference was observed ($p>0.05$) when group 1 day 07 result was compared with result of rest of the groups excluding group 2.

INFLAMMATORY MARKERS		GROUP OF ANIMALS							
		01	02	03	04	05	06	07	08
		ng/ml							
IL6	DAY03	0.32±0.02	0.75±0.02	0.32±0.03	0.32±0.04	0.73±0.05	0.75±0.04	0.74±0.02	0.76±0.06
	DAY07	0.33±0.04	0.98±0.05	0.33±0.04	0.33±0.03	0.34±0.05	0.35±0.04	0.33±0.02	0.76±0.06
IL8	DAY03	0.42±0.03	0.78±0.02	0.41±0.04	0.42±0.03	0.91±0.05	0.92±0.02	0.97±0.03	0.96±0.04
	DAY07	0.43±0.04	0.98±0.05	0.43±0.06	0.44±0.05	0.41±0.04	0.43±0.03	0.40±0.05	0.42±0.02
IL10	DAY03	0.22±0.04	0.46±0.05	0.23±0.03	0.22±0.04	0.45±0.03	0.47±0.03	0.43±0.03	0.42±0.05
	DAY07	0.21±0.03	0.58±0.04	0.22±0.04	0.23±0.02	0.39±0.03	0.37±0.04	0.38±0.02	0.36±0.04
TNFα	DAY03	0.42±0.04	2.24±0.07	0.41±0.05	0.42±0.04	2.23±0.07	2.25±0.08	2.24±0.05	2.26±0.08
	DAY07	0.43±0.05	3.12±0.08	0.42±0.07	0.41±0.06	0.42±0.05	0.43±0.06	0.41±0.08	0.43±0.07
HISTAMINE	DAY03	42±3.9	75±3.8	41±4.1	42±4.3	77±4.0	78±3.8	80±3.7	76±3.5
	DAY07	43±4.5	149±4.9	42±4.2	43±4.0	43±3.9	42±3.4	41±4.8	44±3.7
		µg/ml							
C-REACTIVE PROTEIN	DAY03	341±25	701±28	340±33	341±35	784±23	720±36	761±32	735±22
	DAY07	345±27	1100±33	342±36	343±23	342±28	344±30	345±21	343±25

Table 7: Group-wise change of inflammatory markers measured in day 03 and day 07. The data are the average of three experiments ± SD.

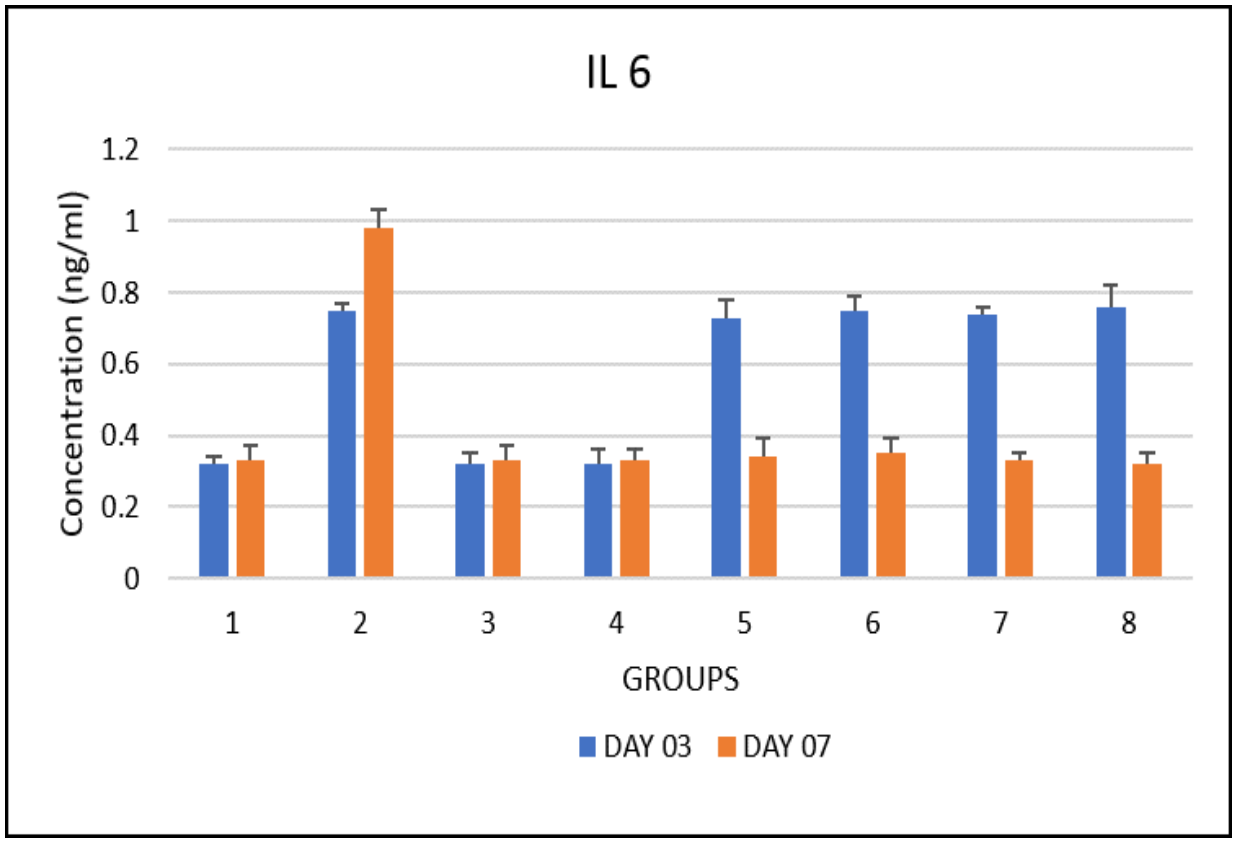
IL 6
Concentration (ng/ml)
1.2
1
0.8
0.6
0.4
0.2
0
1
2
3
4
5
6
7
8
GROUPS
DAY 03
DAY 07

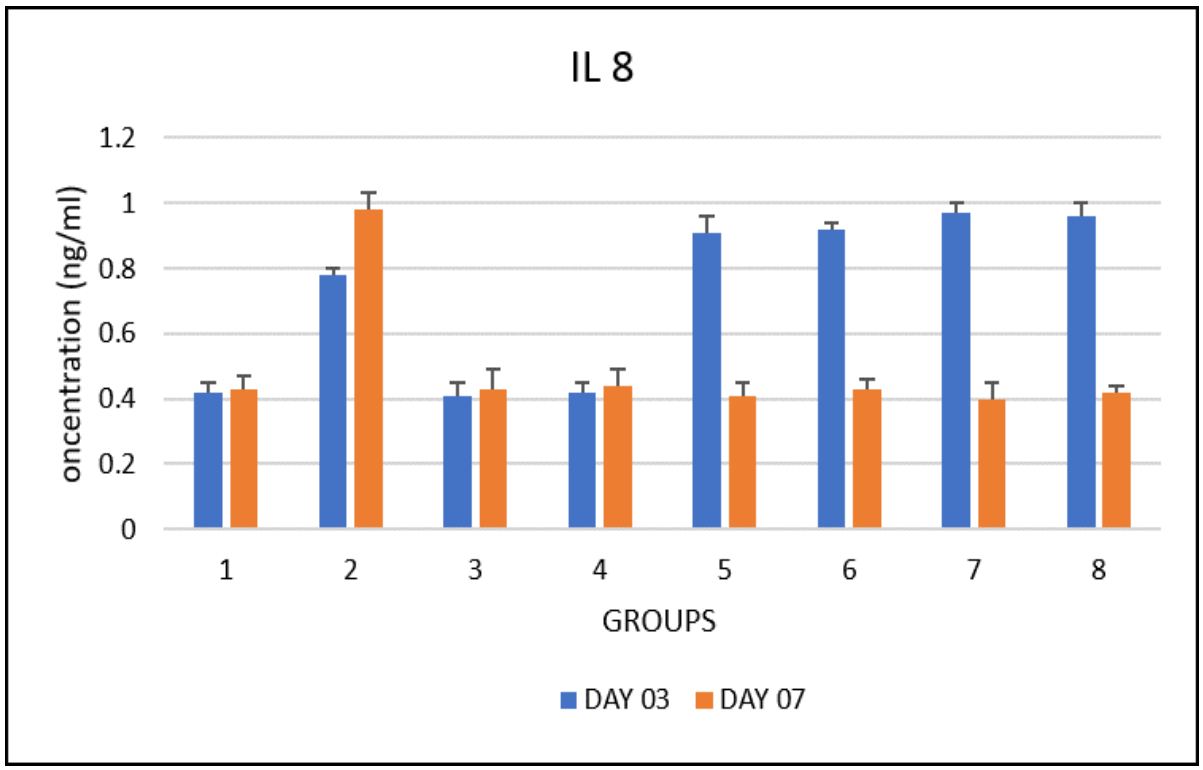
IL 8
oncentration (ng/ml)
1.2
1
0.8
0.6
0.4
0.2
0
1
2
3
4
5
6
7
8
GROUPS
DAY 03
DAY 07

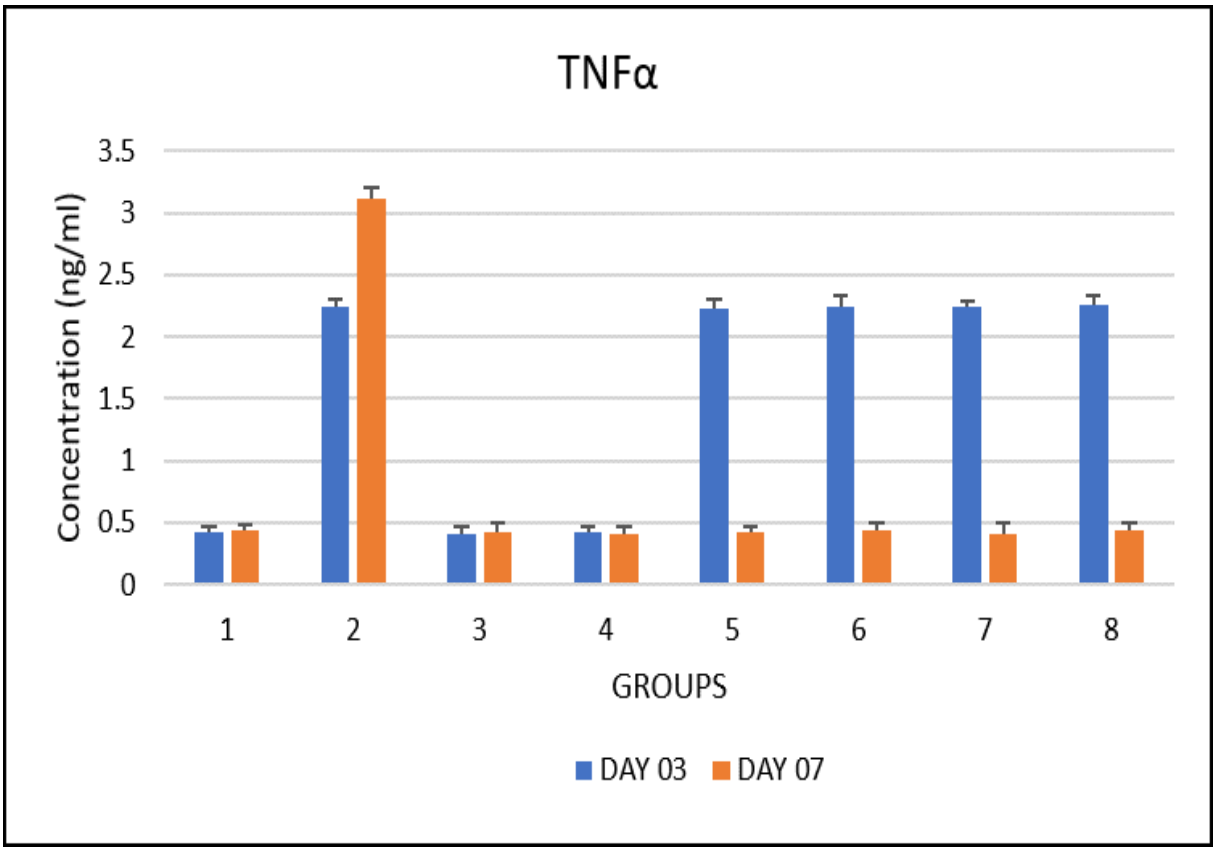
TNFα
Concentration (ng/ml)
3.5
3
2.5
2
1.5
1
0.5
0
1
2
3
4
5
6
7
8
GROUPS
DAY 03
DAY 07

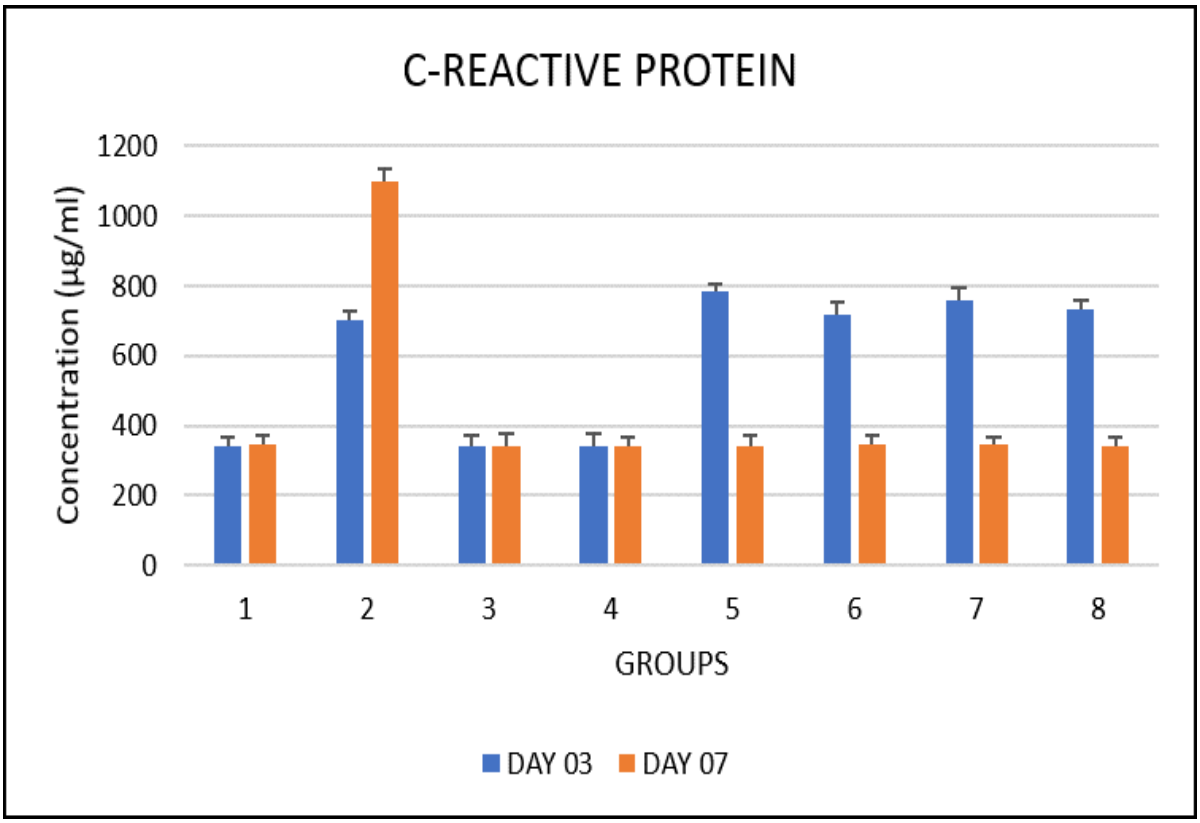
C-REACTIVE PROTEIN
Concentration (µg/ml)
1200
1000
800
600
400
200
0
1
2
3
4
5
6
7
8
GROUPS
DAY 03
DAY 07

Figure 18 Study of pro-inflammatory cytokines. The data are the average of three experiments ± SD.

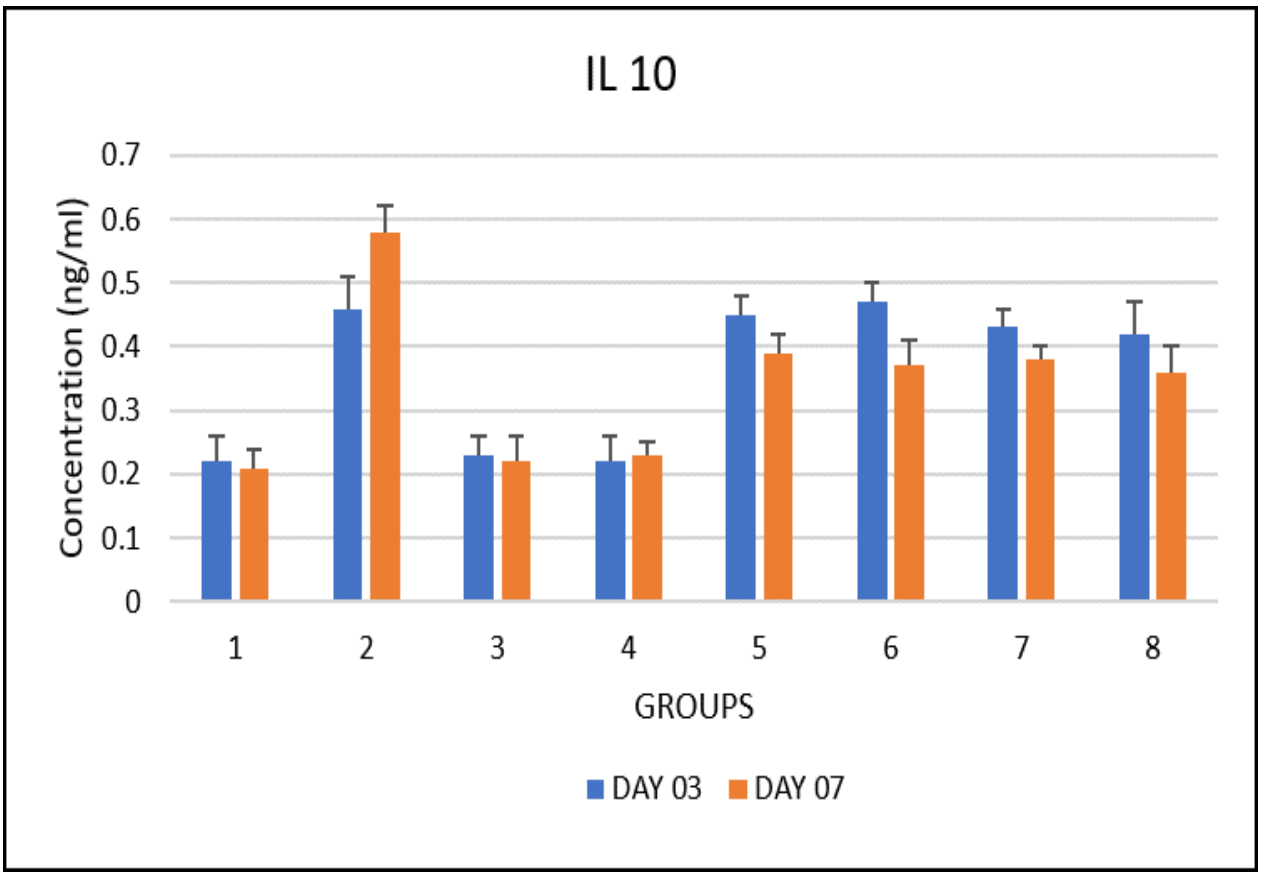

Figure 19 Study of anti-inflammatory cytokine. The data are the average of three experiments ± SD.

Observed changes in cytokine modulator

From the given figure (20), it can be concluded that, serum histamine level was increased due to *S. aureus*, which gradually decreased at the end of the treatment (day 7). No statistically significant difference was observed ($p>0.05$) when group 1 day 07 result was compared with result of rest of the groups excluding group 2.

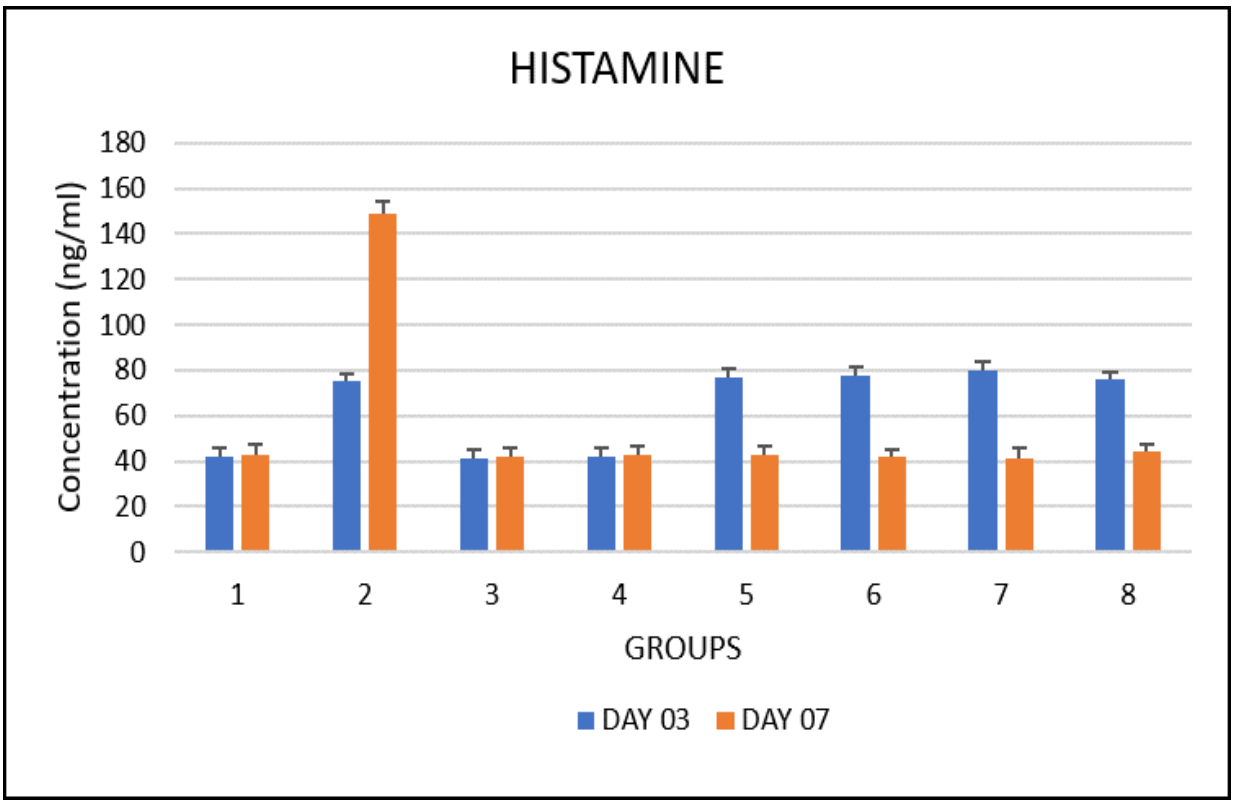

Figure 20: Study of cytokine modulator. The data are the average of three experiments ± SD.

Histological Observations

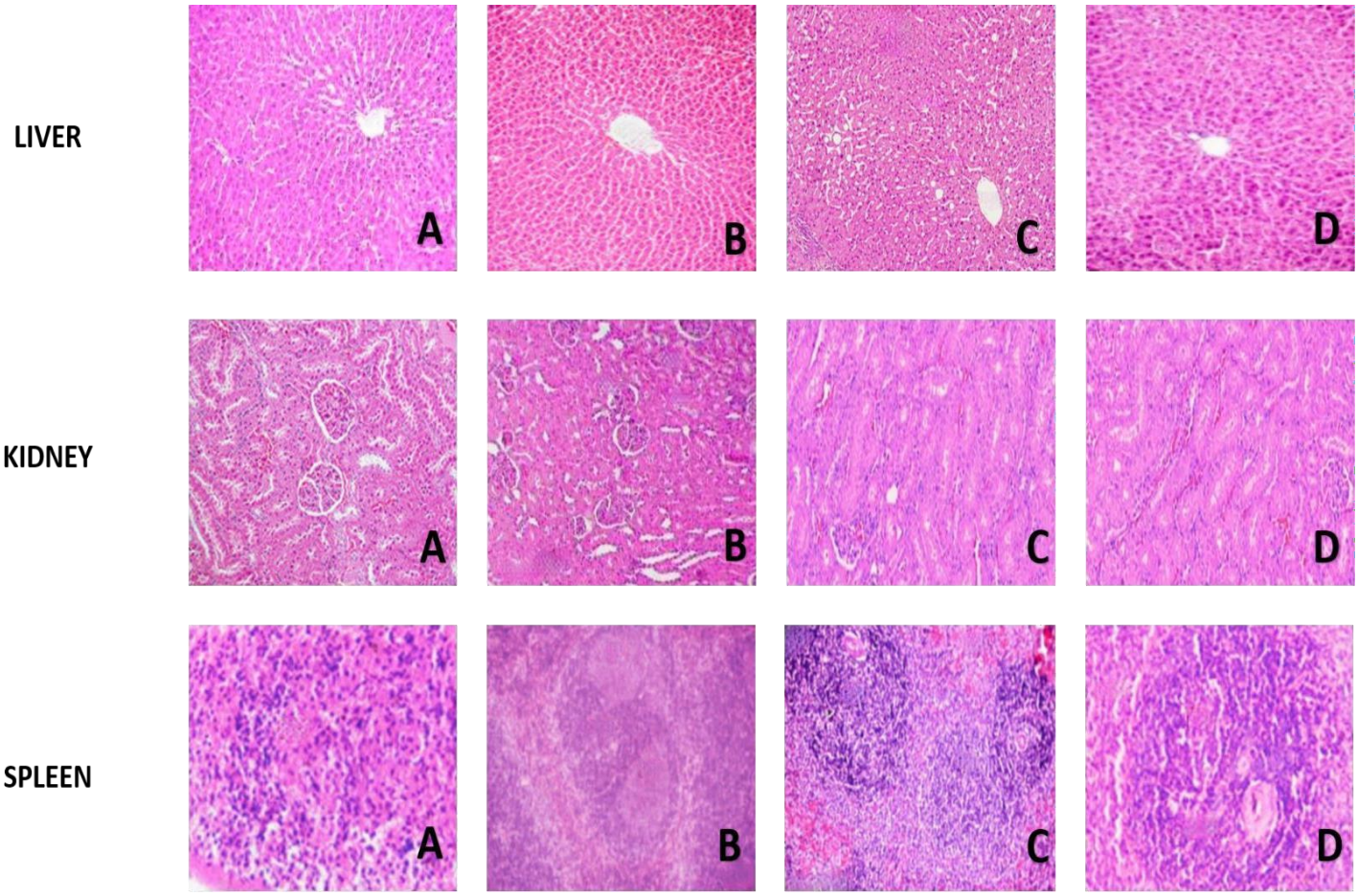

Figure 21: Representative histological study images of selected organs. A=Group 1; B=Group 2; C=Group 3 and D=Group 5.

The tissue sections of nanoparticle exposed groups as observed microscopically and analyzed, revealed no noticeable anomaly when compared with the control group (Figure:21). Thus, it may be concluded that, selected tissues if exposed (in vivo) to specific concentrations of ZnONPs for a limited time are incapable of producing countable necrosis or degeneration.

VI. Conclusion/ Discussion

This study was aimed to compare the therapeutic potential of chemically synthesized commercially available and green synthesized ZnONPs both in *in-vitro* and *in-vivo* models. The use of green synthesis method in this study indicates a strong support to the factor of environmental safety [72]. Moreover, as per the published reports, green synthesized ZnONPs are having a higher bio-compatibility in comparison to chemically synthesized one [73]. Hence, it can be concluded that, experimentation with higher concentrations of green synthesized ZnONPs comparable to the concentrations used in the present study, in case of *in-vivo* models, will not be marked as the major problem in relation to chemo-therapeutic usage of green ZnONPs. As per the results obtained from the *in-vitro* study, which was conducted with both control and multiple-antibiotic-resistant clinical strain of *S. aureus* (ATCC25923 and KC-02), green synthesized ZnONPs showed higher bactericidal effect compared to the commercially available ZnONPs. This finding is in alliance with already reported results [12]. In case of *in-vivo* study, inflammation development was possible by using clinical strain of *S. aureus* (KC-02) [74]. Finding includes almost no change of erythrocytic and leukocytic count post-exposure to both types of ZnONPs (commercial and green synthesized) in the *in-vivo* model. Additionally, the erythrocytic membrane showed no sign of fragility, post-exposure to both the ZnONPs (commercial and green synthesized). This helps to conclude, both types of ZnONPs, when used in the mentioned concentrations (alone or in combination with antibiotic) were harmless to the principal cellular elements of blood. Although, reactive oxygen species generating ability of ZnONPs should affect least the RBCs [75], but according to proposals forwarded by a number of published reports, chemically synthesized ZnONPs may act as a factor for increasing the fragility of erythrocytic membrane [76]. But the results of the current study are not in agreement with these proposals, probably due to the particular concentrations used. Literature findings, till date, do not suggest the existence of such detrimental ability in case of green synthesized ZnONPs [77]. The development of inflammation in the *S. aureus* injected groups was indicated by the serum level of inflammatory markers. On the other hand, normal serum level of inflammatory markers observed in group 3 and 4 clearly indicates, both the ZnONPs were incapable of inducing inflammation [78]. According to the published reports, the onset of inflammation in almost each and every type of inflammatory disease, is marked by the rise in serum level of pro-inflammatory markers (IL-6,8, TNFα, C-reactive protein), followed by its decline, compensated

by the rise in serum level of anti-inflammatory marker (IL-10) [79]. In case of this study, the observed changes in the pattern of serum level of both pro-inflammatory and anti-inflammatory markers during the development and termination of inflammation are in complete agreement to the reported trend. Increased secretion of pro-inflammatory marker IL-6 acts as initiating signal, enhancing the levels of acute phase proteins including C-Reactive protein, as observed in case of acute sepsis [80]. This increased level of C-Reactive protein is then responsible for increasing the IL-8 level via reactive oxygen species formation with the help of NAD(P)H oxidase [81]. On the other hand, higher levels of TNFα acts as a strong signal that results in higher secretion of IL- 6 [82], further enhancing the serum levels of C-Reactive proteins and IL-8. Next, the increased level of TNFα is capable of initiating higher secretion of IL-10 by macrophages mainly [83]. This enhanced level of IL-10, mostly observed when the inflammation reaches a maximum as per the magnitude of the inducing signal, acts in a negative feedback pattern and dampen the inflammatory response by inhibiting the secretion of IL-6 [84]. Besides, the observed changes in the level of serum cytokine modulator (Histamine) showed no deviation from the reported results [85]. It was also observed that, similar pattern of changes in the serum level of inflammatory markers were achieved when combination of antibiotic and ZnONPs were administered in place of only ZnONPs. Besides, inhibiting the inflammation, the ZnONPs (both commercial and green synthesized) caused no noticeable histological change in vital organs (liver, kidney, spleen and adrenal gland), when used in the mentioned concentrations. The entire study also supports the fact that, ZnONPs showed selective toxicity to prokaryotic cells, leading to its potential damage, leaving eukaryotic cells intact, within a certain biological limit.

VII. Significance of the study

1. Green ZnONPs was successfully synthesized following easy-to-use protocol using coriander leaves.
2. A number of characterization methods (XRD, DLS etc.) were implemented for investigating the properties of green synthesized ZnONPs, following its comparison with chemically synthesized commercially available ZnONPs.
3. The characterization process helps to identify that, green ZnONPs was almost similar in morphology and size like the commercially available ZnONPs.
4. Green synthesized ZnONPs showed higher bactericidal effect than chemically synthesized commercially available one.
5. Clinical strain (KC-02) was confirmed to a strain of *S. aureus.*
6. Both ZnONPs (commercial and green synthesized) were suitable for implementing synergistic effect to inhibit bacterial growth, when used in combination with antibiotic.
7. The inflammatory model was successfully developed by using the clinical strain (KC-02) of *S. aureus.*
8. Compared to chemically synthesized commercially available ZnONPs, lower concentration of green synthesized ZnONPs was capable of inhibiting inflammation.
9. Almost equal magnitude of anti-inflammatory response was showed both by combinations (ZnONPs and antibiotic) and individual ZnONPs.
10. Both the ZnONPs were harmless to blood cells and organs like liver, kidney, spleen and adrenal glands in *in-vivo* condition.

VIII. Future Directions

This study can be used as a foundation for establishing new line of antibacterial and anti-inflammatory chemotherapeutics. Further in-vivo research is required to target green synthesized ZnONPs to specific organs, in order to evaluate organ-specific functionalities without interfering with the general physiology of the organism. If this line of work gets established, human trials will be the final step for the administration of ZnONPs for combating infections occurring from multiple antibiotic resistant pathogenic bacteria and also ameliorating the pathogen-induced inflammatory response.

IX. References

1. Xu, J., Hu, Y., Wang, S., Ma, X., & Guo, J. (2020). Nanomaterials in electrochemical cytosensors. *Analyst*, *145*(6), 2058-2069.

2. Kuruppu, K. A. S. S., Perera, K. M. K. G., Chamara, A. M. R., & Thiripuranathar, G. (2020). Flower shaped ZnO—NPs; phytofabrication, photocatalytic, fluorescence quenching, and photoluminescence activities. *Nano Express*, *1*(2), 020020.

3. Gupta, M. K., Tandon, P. K., & Shukla, N. (2019). Nanotechnology: Environmentally Sustainable Solutions for Water Treatment. In *Nanostructured Materials for Treating Aquatic Pollution* (pp. 225-242). Springer, Cham.

4. Wang, C. Y., Makvandi, P., Zare, E. N., Tay, F. R., & Niu, L. N. (2020). Advances in antimicrobial organic and inorganic nanocompounds in biomedicine. *Advanced Therapeutics*, *3*(8), 2000024.

5. Aswathy, R., Gabylis, B., Anwesha, S., & Bhaskara Rao, K. (2017). Green synthesis and characterization of marine yeast-mediated silver and zinc oxide nanoparticles and assessment of their antioxidant activity. *Asian Journal of Pharmaceutical and Clinical Research*, *10*(10), 235-240.

6. Gowdhami, B., Jaabir, M., Archunan, G., & Suganthy, N. (2019). Anticancer potential of zinc oxide nanoparticles against cervical carcinoma cells synthesized via biogenic route using aqueous extract of Gracilaria edulis. *Materials Science and Engineering: C*, *103*, 109840.

7. Rautela, A., Rani, J., & Das, M. D. (2019). Green synthesis of silver nanoparticles from Tectona grandis seeds extract: characterization and mechanism of antimicrobial action on different microorganisms. *Journal of Analytical Science and Technology*, *10*(1), 1-10.

8. Mensch, A. C., Hernandez, R. T., Kuether, J. E., Torelli, M. D., Feng, Z. V., Hamers, R. J., & Pedersen, J. A. (2017). Natural organic matter concentration impacts the interaction of functionalized diamond nanoparticles with model and actual bacterial membranes. *Environmental science & technology*, *51*(19), 11075-11084.

9. Shariatinia, Z., & Mohammadi-Denyani, A. (2018). Advances in polymers for drug delivery and wound healing applications. *Advances in polymers for biomedical applications*, 85-141.

10. Pillai, A. M., Sivasankarapillai, V. S., Rahdar, A., Joseph, J., Sadeghfar, F., Rajesh, K., & Kyzas, G. Z. (2020). Green synthesis and characterization of zinc oxide nanoparticles with antibacterial and antifungal activity. *Journal of Molecular Structure, 1211*, 128107.

11. Kalita, C., Tudu, B., & Saikia, P. (2021). Synthesis of Novel Metal/Metal Oxide-Based Nanomaterials Using Plant Derivatives and Their Potential Environmental Applications. In *Biobased Nanotechnology for Green Applications* (pp. 557-584). Springer, Cham.

12. Pal, S., Pal, K., Mukherjee, S., Bera, D., Karmakar, P., & Sukhen, D. (2020). Green cardamom mediated phytosynthesis of ZnONPs and validation of its antibacterial and anticancerous potential. *Materials Research Express*, *7*(1), 015068.

13. Aldeen, T. S., Mohamed, H. E. A., & Maaza, M. (2022). ZnO nanoparticles prepared via a green synthesis approach: Physical properties, photocatalytic and antibacterial activity. *Journal of Physics and Chemistry of Solids*, *160*, 110313.

14. Yuliarto, B., Septiani, N. L. W., Kaneti, Y. V., Iqbal, M., Gumilar, G., Kim, M., ... & Yamauchi, Y. (2019). Green synthesis of metal oxide nanostructures using naturally occurring compounds for energy, environmental, and bio-related applications. *New Journal of Chemistry*, *43*(40), 15846-15856.

15. Shil, A., Mukherjee, S., Bishayi, B., & Sikdar (Nee) Bhakta, M. (2021). A Comparison of Antibacterial Effects of Catharanthus roseus and Camellia sinensis (Black Tea) and Their Synergistic Effect along with Antibiotic against Multiple Antibiotic Resistant Strains of Staphylococcus aureus. *Journal of Herbs, Spices & Medicinal Plants*, *27*(2), 135-148.

16. Otong, E. S., & Musa, S. A. (2019). Antioxidant potentials of Miyan Kuka (Baobab leaves). *Annals of African Medical Research*, *2*(1).

17. El-Seedi, H. R., El-Shabasy, R. M., Khalifa, S. A., Saeed, A., Shah, A., Shah, R., ... & Guo, W. (2019). Metal nanoparticles fabricated by green chemistry using natural extracts: biosynthesis, mechanisms, and applications. *RSC advances*, *9*(42), 24539-24559.

18. Teng, F., Liu, X., Guo, S. B., Li, Z., Ji, W. Q., Zhang, F., & Zhu, X. M. (2019). Community-acquired bacterial co-infection predicts severity and mortality in influenza-associated pneumonia admitted patients. *Journal of infection and chemotherapy*, *25*(2), 129-136.

19. Boswihi, S. S., & Udo, E. E. (2018). Methicillin-resistant Staphylococcus aureus: An update on the epidemiology, treatment options and infection control. *Current Medicine Research and Practice*, *8*(1), 18-24.

20. Alfaro-Gonzalez, B., Ulate, D., Alvarado, R., & Argüello-Miranda, O. (2018). Chitosan-silver nanoparticles as an approach to control bacterial proliferation, spores and antibiotic-resistant bacteria. *Biomedical Physics & Engineering Express*, *4*(3), 035011.

21. Pumipuntu, N., Kulpeanprasit, S., Santajit, S., Tunyong, W., Kong-Ngoen, T., Hinthong, W., & Indrawattana, N. (2017). Screening method for Staphylococcus aureus

identification in subclinical bovine mastitis from dairy farms. *Veterinary world*, *10*(7), 721.

22. A Abbas, H., H Shaker, G., AH Hegazy, W., & A Baiomy, A. (2018). Prevalence of multi-drug resistant Staphylococci isolated from surgical site infections. *Zagazig Journal of Pharmaceutical Sciences*, *27*(1), 31-38.

23. El-Halfawy, O. M., & Valvano, M. A. (2011). Heteroresistance of opportunistic bacteria to antimicrobial peptides: a new challenge to antimicrobial therapy of cystic fibrosis infections. *Clinical Practice*, *8*(6), 591.

24. Chen, X., Gu, X., Bao, L., Ma, S., & Mu, Y. (2021). Comparison of adsorption and desorption of triclosan between microplastics and soil particles. *Chemosphere*, *263*, 127947.

25. Bernardi, L., & Esposito, S. (2020). Update on acute bone and joint infections in paediatrics: a narrative review on the most recent evidence-based recommendations and appropriate antinfective therapy. *Antibiotics*, *9*(8), 486.

26. Jin, T., Mohammad, M., Pullerits, R., & Ali, A. (2021). Bacteria and host interplay in Staphylococcus aureus septic arthritis and sepsis. *Pathogens*, *10*(2), 158.

27. Shaw, T., Tellapragada, C., Ke, V., AuCoin, D. P., & Mukhopadhyay, C. (2018). Performance evaluation of Active Melioidosis Detect-Lateral Flow Assay (AMD-LFA) for diagnosis of melioidosis in endemic settings with limited resources. *PLoS One*, *13*(3), e0194595.

28. Davie-Smith, F., & Carse, B. (2021). Comparison of patient-reported and functional outcomes following transition from mechanical to microprocessor knee in the low-activity user with a unilateral transfemoral amputation. *Prosthetics and Orthotics International*, *45*(3), 198-204.

29. Reyes, M. S., Porro, S., & Pirovani, M. E. (2015). Actitudes hacia la química en estudiantes universitarios conforme avanzan en la carrera. *Revista de la Facultad de Ciencias Químicas*, (11), 70-76.

30. Preston Church, L. W., Chopra, A., & Judson, M. A. (2017). Paradoxical Reactions and the Immune Reconstitution Inflammatory Syndrome. *Tuberculosis and Nontuberculous Mycobacterial Infections*, 637-652.

31. Joshi, P. N., Mathias, A., & Mishra, A. (2018). Synthesis of ecofriendly fluorescent carbon dots and their biomedical and environmental applications. *Materials Technology*, *33*(10), 672-680.

32. Andres-Verges, M., & Martinez-Gallego, M. (1992). Spherical and rod-like zinc oxide microcrystals: morphological characterization and microstructural evolution with temperature. *Journal of materials science*, *27*(14), 3756-3762.

33. Satdeve, N. S., Ugwekar, R. P., & Bhanvase, B. A. (2019). Ultrasound assisted preparation and characterization of Ag supported on ZnO nanoparticles for visible light degradation of methylene blue dye. *Journal of Molecular Liquids*, *291*, 111313.

34. Khan, M. M., Harunsani, M. H., Tan, A. L., Hojamberdiev, M., Poi, Y. A., & Ahmad, N. (2020). Antibacterial studies of ZnO and Cu-doped ZnO nanoparticles synthesized using aqueous leaf extract of Stachytarpheta jamaicensis. *BioNanoScience*, *10*(4), 1037-1048.

35. Sharma, S., & Uttam, K. N. (2017). Rapid analyses of stress of copper oxide nanoparticles on wheat plants at an early stage by laser induced fluorescence and attenuated total reflectance Fourier transform infrared spectroscopy. *Vibrational Spectroscopy*, *92*, 135-150.

36. Nithya, K., & Kalyanasundharam, S. (2019). Effect of chemically synthesis compared to biosynthesized ZnO nanoparticles using aqueous extract of C. halicacabum and their antibacterial activity. *OpenNano*, *4*, 100024.

37. Norouzzadeh, P., Mabhouti, K., Golzan, M. M., & Naderali, R. (2020). Investigation of structural, morphological and optical characteristics of Mn substituted Al-doped ZnO NPs: A Urbach energy and Kramers-Kronig study. *Optik*, *204*, 164227.

38. Bayat, M., Chudinova, E., Zargar, M., Lyashko, M., Louis, K., & Adenew, F. K. (2019). Phyto-assisted green synthesis of zinc oxide nanoparticles and its antibacterial and antifungal activity. *Research on Crops*, *20*(4), 725-730.

39. Barzinjy, A. A., & Azeez, H. H. (2020). Green synthesis and characterization of zinc oxide nanoparticles using Eucalyptus globulus Labill. leaf extract and zinc nitrate hexahydrate salt. *SN Applied Sciences*, *2*(5), 1-14.

40. Wang, W., Wang, Y., Lin, L., Song, Y., & Yang, C. J. (2019). A tridecaptin-based fluorescent probe for differential staining of Gram-negative bacteria. *Analytical and bioanalytical chemistry*, *411*(18), 4017-4023.

41. Tajabadi, N., Mardan, M., Shuhaimi, M., & Manap, M. A. (2011). Isolation and identification of Enterococcus sp. from honey stomach of honeybee based on biochemical and 16S rRNA sequencing analysis. *International Journal of Probiotics & Prebiotics*, *6*(2), 95.

42. Baharuddin, A. (2019). Polymerase Chain Reaction (PCR) Method for Identification Gene Escherichia coli and Officer Depot Behavior in Drinking Water Refill. *Executive Editor*, *10*(1), 315.

43. Kluesner, M. G., Nedveck, D. A., Lahr, W. S., Garbe, J. R., Abrahante, J. E., Webber, B. R., & Moriarity, B. S. (2018). EditR: a method to quantify base editing from Sanger sequencing. *The CRISPR journal*, *1*(3), 239-250.

44. Musa, H., Kasim, F. H., Gunny, A. A. N., & Gopinath, S. C. (2018). Salt-adapted moulds and yeasts: Potentials in industrial and environmental biotechnology. *Process Biochemistry*, *69*, 33-44.

45. Vaishali, M., & Geetha, R. V. (2018). Antibacterial activity of Orange peel oil on Streptococcus mutans and Enterococcus-An In-vitro study. *Research Journal of Pharmacy and Technology*, *11*(2), 513-514.

46. Naimi-Shamel, N., Pourali, P., & Dolatabadi, S. (2019). Green synthesis of gold nanoparticles using Fusarium oxysporum and antibacterial activity of its tetracycline conjugant. *Journal de mycologie medicale*, *29*(1), 7-13.

47. El-Saadony, M. T., Sitohy, M. Z., Ramadan, M. F., & Saad, A. M. (2021). Green nanotechnology for preserving and enriching yogurt with biologically available iron (II). *Innovative Food Science & Emerging Technologies*, *69*, 102645.

48. Trigo-Gutierrez, J. K., Vega-Chacón, Y., Soares, A. B., & Mima, E. G. D. O. (2021). Antimicrobial Activity of Curcumin in Nanoformulations: A Comprehensive Review. *International Journal of Molecular Sciences*, *22*(13), 7130.

49. Muthuvel, A., Jothibas, M., & Manoharan, C. (2020). Effect of chemically synthesis compared to biosynthesized ZnO-NPs using Solanum nigrum leaf extract and their photocatalytic, antibacterial and in-vitro antioxidant activity. *Journal of Environmental Chemical Engineering*, *8*(2), 103705.

50. Enan, E. T., Ashour, A. A., Basha, S., Felemban, N. H., & El-Rab, S. M. G. (2021). Antimicrobial activity of biosynthesized silver nanoparticles, amoxicillin, and glass-ionomer cement against Streptococcus mutans and Staphylococcus aureus. *Nanotechnology*, *32*(21), 215101.

51. Perez, M. G., Fourcade, L., Mateescu, M. A., & Paquin, J. (2017). Neutral Red versus MTT assay of cell viability in the presence of copper compounds. *Analytical biochemistry*, *535*, 43-46.

52. Tiwari, R. K., Singh, S., Gupta, C. L., Pandey, P., Singh, V. K., Sayyed, U., ... & Bajpai, P. (2021). Repolarization of glioblastoma macrophage cells using non-agonistic Dectin-1

ligand encapsulating TLR-9 agonist: plausible role in regenerative medicine against brain tumor. *International Journal of Neuroscience*, *131*(6), 591-598.

53. Ghosh, S., & Bandyopadhyay, P. K. (2019). Molecular characterization of newly identified Klebsiella PKBSG14 and analysis of its effect on immune response and cell cycle progression using common catfish (Channa punctatus) as a model. *Microbial pathogenesis*, *127*, 368-379.

54. Husain, F. M., Ansari, A. A., Khan, A., Ahmad, N., Albadri, A., & Albalawi, T. H. (2019). Mitigation of acyl-homoserine lactone (AHL) based bacterial quorum sensing, virulence functions, and biofilm formation by yttrium oxide core/shell nanospheres: Novel approach to combat drug resistance. *Scientific reports*, *9*(1), 1-10.

55. Nejabatdoust, A., Salehzadeh, A., Zamani, H., & Moradi-Shoeili, Z. (2019). Synthesis, characterization and functionalization of ZnO nanoparticles by glutamic acid (Glu) and conjugation of ZnO@ Glu by thiosemicarbazide and its synergistic activity with ciprofloxacin against multi-drug resistant Staphylococcus aureus. *Journal of Cluster Science*, *30*(2), 329-336.

56. Biswas, S., & Kumar Mukhopadhyay, P. (2020). Casein-and pea-enriched high-protein diet can take care of the reprotoxic effects of arsenic in male rats. *Andrologia*, *52*(5), e13560.

57. Zhang, L., Chen, Z. W., Yang, S. F., Shaer, M., Wang, Y., Dong, J. J., & Jiapaer, B. (2019). MicroRNA-219 decreases hippocampal long-term potentiation inhibition and hippocampal neuronal cell apoptosis in type 2 diabetes mellitus mice by suppressing the NMDAR signaling pathway. *CNS neuroscience & therapeutics*, *25*(1), 69.

58. Yokota, J., & Kyotani, S. (2018). Influence of nanoparticle size on the skin penetration, skin retention and anti-inflammatory activity of non-steroidal anti-inflammatory drugs. *Journal of the Chinese Medical Association*, *81*(6), 511-519.

59. Sanabria, A., Røkeberg, M. E., Johannessen, M., Sollid, J. E., Simonsen, G. S., & Hanssen, A. M. (2019). Culturing periprosthetic tissue in BacT/Alert® Virtuo blood culture system leads to improved and faster detection of prosthetic joint infections. *BMC infectious diseases*, *19*(1), 1-8.

60. Billman, Z. P., Kas, A., Stone, B. C., & Murphy, S. C. (2016). Defining rules of CD8+ T cell expansion against pre-erythrocytic Plasmodium antigens in sporozoite-immunized mice. *Malaria journal*, *15*(1), 1-13.

61. Niu, Z., Zhang, W., Yu, C., Zhang, J., & Wen, Y. (2018). Recent advances in biological sample preparation methods coupled with chromatography, spectrometry and

electrochemistry analysis techniques. *TrAC Trends in Analytical Chemistry*, *102*, 123-146.

62. Liu, Y., Goldfarb, D. S., El-Achkar, T. M., Lieske, J. C., & Wu, X. R. (2018). Tamm-Horsfall protein/uromodulin deficiency elicits tubular compensatory responses leading to hypertension and hyperuricemia. *American Journal of Physiology-Renal Physiology*, *314*(6), F1062-F1076.

63. Ohlsson, P., Petersson, K., Augustsson, P., & Laurell, T. (2018). Acoustic impedance matched buffers enable separation of bacteria from blood cells at high cell concentrations. *Scientific reports*, *8*(1), 1-11.

64. Zhao, K. N., Dimeski, G., De Jersey, J., Johnson, L. A., Grant, M., Masci, P. P., & Lavin, M. F. (2019). Next-generation rapid serum tube technology using prothrombin activator coagulant: fast, high-quality serum from normal samples. *Clinical Chemistry and Laboratory Medicine (CCLM)*, *57*(4), 483-497.

65. Osikoya, I. O., Afolabi, I. S., Okafor, A., & Rotimi, S. O. (2017). Antioxidant Activity of Solenostemon monostachyus (P. Beauv.) Briq. in Induced Rats. *International Journal of Biochemistry Research & Review*, *18*(4), 1-11.

66. Hun, X., & Kong, X. (2021). An enzyme linked aptamer photoelectrochemical biosensor for Tau-381 protein using AuNPs/MoSe2 as sensing material. *Journal of Pharmaceutical and Biomedical Analysis*, *192*, 113666.

67. Kumar, R., Gupta, A., Singh, A. K., Bishayee, A., & Pandey, A. K. (2020). The Antioxidant and Antihyperglycemic Activities of Bottlebrush Plant (Callistemon lanceolatus) Stem Extracts. *Medicines*, *7*(3), 11.

68. Ji, P., Gong, Y., & Hu, X. (2019). Role of PD-1/PD-L1 in microenvironment of breast cancer. *Zhonghua zhong liu za zhi [Chinese journal of oncology]*, *41*(6), 401-405.

69. Safhi, M. M., Anwer, T., Khan, G., Siddiqui, R., Sivakumar, S. M., & Alam, M. F. (2018). The combination of canagliflozin and omega-3 fatty acid ameliorates insulin resistance and cardiac biomarkers via modulation of inflammatory cytokines in type 2 diabetic rats. *The Korean Journal of Physiology & Pharmacology*, *22*(5), 493-501.

70. Rupa, P., & Mine, Y. (2019). Comparison of glycated ovalbumin–monosaccharides in the attenuation of ovalbumin-induced allergic response in a BALB/C mouse model. *Journal of agricultural and food chemistry*, *67*(29), 8138-8148.

71. Chakrabarti, S., Islam, J., Hazarika, H., Mazumder, B., Raju, P. S., & Chattopadhyay, P. (2018). Safety profile of silver sulfadiazine-bFGF-loaded hydrogel for partial thickness burn wounds. *Cutaneous and ocular toxicology*, *37*(3), 258-266.

72. Goutam, S. P., Saxena, G., Singh, V., Yadav, A. K., Bharagava, R. N., & Thapa, K. B. (2018). Green synthesis of TiO2 nanoparticles using leaf extract of Jatropha curcas L. for photocatalytic degradation of tannery wastewater. *Chemical Engineering Journal*, *336*, 386-396.

73. Shah, N. I., Jabeen, N., Irum, S., Ahmad, K. S., Tauseef, I., Khan, T. F., ... & Hussain, S. Z. (2021). Environmentally benign and economical bio-fabrication of ZnO and Cr-doped ZnO nanoparticles using leaf extract of Citrus reticulata for biological activities. *Materials Today Communications*, *27*, 102383.

74. Baranwal, G., Mohammad, M., Jarneborn, A., Reddy, B. R., Golla, A., Chakravarty, S., ... & Biswas, R. (2017). Impact of cell wall peptidoglycan O-acetylation on the pathogenesis of Staphylococcus aureus in septic arthritis. *International Journal of Medical Microbiology*, *307*(7), 388-397.

75. Bagchi, D., Rathnam, V. S., Lemmens, P., Banerjee, I., & Pal, S. K. (2018). NIR-Light-active ZnO-based nanohybrids for bacterial biofilm treatment. *ACS omega*, *3*(9), 10877-10885.

76. Xie, L., Zhang, Y., Gao, J., Li, X., & Wang, H. (2020). Nitrate exposure induces intestinal microbiota dysbiosis and metabolism disorder in Bufo gargarizans tadpoles. *Environmental Pollution*, *264*, 114712.

77. Mohamed, A. A., Fouda, A., Abdel-Rahman, M. A., Hassan, S. E. D., El-Gamal, M. S., Salem, S. S., & Shaheen, T. I. (2019). Fungal strain impacts the shape, bioactivity and multifunctional properties of green synthesized zinc oxide nanoparticles. *Biocatalysis and Agricultural Biotechnology*, *19*, 101103.

78. Liu, J., Feng, X., Wei, L., Chen, L., Song, B., & Shao, L. (2016). The toxicology of ion-shedding zinc oxide nanoparticles. *Critical reviews in toxicology*, *46*(4), 348-384.

79. Donath, M. Y. (2014). Targeting inflammation in the treatment of type 2 diabetes: time to start. *Nature reviews Drug discovery*, *13*(6), 465-476.

80. Bui, T. T., Piao, C. H., Kim, S. M., Song, C. H., Shin, H. S., Lee, C. H., & Chai, O. H. (2017). Citrus tachibana leaves ethanol extract alleviates airway inflammation by the modulation of Th1/Th2 imbalance via inhibiting NF-κ B signaling and histamine secretion in a mouse model of allergic asthma. *Journal of medicinal food*, *20*(7), 676-684.

81. Poe, F. L., & Corn, J. (2020). N-Acetylcysteine: A potential therapeutic agent for SARS-CoV-2. *Medical hypotheses*, *143*, 109862.

82. Noack, M., Beringer, A., & Miossec, P. (2019). Additive or synergistic interactions between IL-17A or IL-17F and TNF or IL-1β depend on the cell type. *Frontiers in immunology*, *10*, 1726.

83. Atri, C., Guerfali, F. Z., & Laouini, D. (2018). Role of human macrophage polarization in inflammation during infectious diseases. *International journal of molecular sciences*, *19*(6), 1801.

84. Ren, S. S., Xu, L. L., Wang, P., Li, L., Hu, Y. T., Xu, M. Q., ... & Yang, J. Y. (2019, July). Circadian rhythms have effects on surgical outcomes of liver transplantation for patients with hepatocellular carcinoma: A retrospective analysis of 147 cases in a single center. In *Transplantation proceedings* (Vol. 51, No. 6, pp. 1913-1919). Elsevier.

85. Sebbag, L., Allbaugh, R. A., Weaver, A., Seo, Y. J., & Mochel, J. P. (2019). Histamine-induced conjunctivitis and breakdown of blood–tear barrier in dogs: a model for ocular pharmacology and therapeutics. *Frontiers in pharmacology*, *10*, 752.